

國立臺灣大學生物資源暨農學院森林環境暨資源學研究所

碩士論文

School of Forestry and Resource Conservation

College of Bioresources and Agriculture

National Taiwan University

Master Thesis



拉拉山森林動態樣區木本植物組成與環境之關係

Woody Species Composition of the Lalashan Forest

Dynamics Plot and its Relationship to Environment

陳婷

Ting Chen

指導教授：澤大衛 博士 & 鍾國芳 博士

Advisor: David Zelený, Ph.D. & Kuo-Fang Chung, Ph.D.

中華民國 112 年 1 月

January, 2023

誌謝

能夠完成本研究要感謝的人很多，其中又以我的指導教授 David Zelený，李靜峯老師和鍾國芳老師為最，感謝他們在我的碩士生涯中給予我研究及人生上的許多幫助和引導，讓我能夠堅持並完成這段學習生涯及研究。再來要感謝所有植群生態學研究室的成員：建帆、彥成、宗儀、昆松、Jéssica、以諾、碩瑜、信彥、柏佑、冠甫、奕嫩、宗宸、敬麟、晟洋、宇霈、魏碩、書逸、訓宏和尹舜，感謝大家在碩士生涯的教學相長及陪伴與鼓勵，你們是除了老師們以外給予我最多幫助及支持的一群夥伴。當然，能夠順利建立並收完整個拉拉山森林動態樣區的每木資料，來參與調查的所有小工也是功不可沒的一群夥伴；感謝曾經參與過拉拉山森林動態樣區每木調查的聿筠、顥源、瑋慈、馨慧、亮廷、亦欣、妮臻、睿騏、國強、欣澤、根榮、Jennifer、品萱、予佳、韋廷、羅易、柏勳、曉陽、子穎、詠寬和乃容，因為有你們的協助，才能讓我們完成這個浩大的任務。也要感謝在我們需要進行土壤樣本分析時，大方伸出援手的許正一老師以及土壤調查室整治研究室的成員們，協助我們一起完成樣區土壤樣本的分析，讓我們的研究能夠更加完整。另外還要感謝我的口試委員：趙國容老師及林奐宇研究員，感謝您們給我許多專業的建議，讓我的論文能夠更加完善。也十分感謝林試所的張勵婉研究員和我們分享建立蓮華池森林動態樣區的相關經驗，以及新竹林管處和拉拉山生態教育館的林班口人員協助我們安全地進入插天山自然保留區內並給予諸多協助，讓我們能順利蒐集到珍貴的研究資料。有感謝所有在這段期間協助我的森林所及台大的行政人員，謝謝您們盡可能地協助我順利完成所有相關手續。另外，我還想感謝在我就讀碩士期間給予我精神支持朋友們：苡珊、婉馨、崇羽、冠翔和俞君，不論是陪我一起寫論文、為我加油打氣或是溫暖的關心，都是讓我在想放棄時繼續堅持下去的動力。最後，我想感謝我的家人：爸爸、媽媽、妹妹和外婆，成為我最強大的後盾，讓我能按照自己的步伐完成學業，也陪我一起經歷所有不論是擔憂抑或是開心的時刻；還有我的舅舅和舅媽，在關鍵時刻願意用自己的方式拉我一把，讓我能順利完成學業。





摘要

亞熱帶山地雲霧森林是一種台灣獨特的植群類型，因受到規律且高頻的雲霧影響，使山地雲霧森林中的植物需適應空氣濕度高、光線少、氣溫低及土壤中長期缺乏養分的環境。為了詳細地瞭解決定亞熱帶山地雲霧森林植物群落組成的生態過程，本研究於台灣北部插天山自然保留區內，位於近塔曼山-拉拉山鞍部拉拉山側之檜木山地針闊葉混合雲霧森林中設立了拉拉山森林動態樣區(24°42'N, 121°26'E)。

該一公頃樣區設立於 2019 年 7 月，並於 2020 年 8 月完成第一次樣區木本植物普查，普查資料內容包含樣區中所有胸高直徑 ≥ 1 公分木本植物之物種、胸高直徑、位置及編號。同時，也於樣區中蒐集和地形及土壤性質相關之環境因子以供研究分析(其中有些環境因子含樣區中所有樣方之資料，有些則只含樣區中的 25 個取樣樣方之資料)。

第一次拉拉山森林動態樣區木本植物普查共記錄隸屬於 29 科、42 屬、65 種之 5220 株個體，胸高斷面積共為 69.1 平方公尺/公頃。以種的優勢度而言，台灣扁柏(*Chamaecyparis obtusa* var. *formosana*)和台灣杜鵑(*Rhododendron formosanum*)之重要值指數(IVI)皆為 14%、次為槲子櫟(*Quercus sessilifolia*)佔 9%、昆欄樹(*Trochodendron aralioides*)佔 7%、假柃木(*Eurya crenatifolia*)佔 5%，前五優勢樹種之累積重要值指數達 49%。本研究利用雙向指標種分析(TWINSPAN)將樣區森林以 10 公尺×10 公尺之樣方為單位分為三種植群型後，透過變異數分析(ANOVA)測試植群型間環境因子之差異。

薄葉虎皮楠-台灣扁柏型(*Daphniphyllum himalayense* subsp. *macropodum*-*Chamaecyparis obtusa* var. *formosana* type)共佔 74 個樣方，是樣區中主要的植群類型，主要分布於樣區西側及中央寬闊的稜線上。分類至該植群型之樣方擁有相對平緩的地形及酸鹼值較低之土壤，並擁有較高的平均胸高斷面積及較低的密度。小葉石楠-台灣杜鵑型(*Pourthiaea villosa* var. *parvifolia*-*Rhododendron formosanum* type)共佔 20 個樣方，主要分布於樣區東側的迎風坡上，受東北季風的影響最甚。分類至該植群型之樣方之迎風程度高且土壤酸鹼值高，並擁有較低的平均胸高斷面積及較高的密度及物種豐富度。狹瓣八仙花-假柃木型(*Hydrangea angustipetala*-*Eurya crenatifolia* type)相對較少、僅佔 6 個樣方，主要分布於樣區西側的溪谷中。分類至

該植群型之樣方普遍坡度較陡、地勢較低窪、土壤含石率及土壤酸鹼值高，且擁有所有植群型中最低的密度。

為了瞭解樣區形成現今木本植物物種組成背後的主要成因，我們使用降趨對應分析(DCA)，並將所有通過測試、與樣區物種組成具有顯著相關之環境因子陳列於圖中。DCA 的結果顯示拉拉山森林動態樣區之木本物種組成主要受 DCA 之第一及第二軸所影響。於該分析中可以見得第一軸和海拔及土壤化學性質包含碳氮比、磷、鎂、鋅呈正相關，而和坡度及土壤酸鹼值呈負相關。第二軸則和土壤含石率呈正相關，並和迎風程度、凹凸度及土壤分解中的穩定因子呈負相關。其中，樣區中的木本植物物種組成主要於擁有較高土壤酸鹼度之較陡的迎風坡和擁有較低土壤酸鹼度之平坦且較高之稜線間發生變化。而次要的物種組成變化則發生於擁有較高凹凸度之地形及擁有較低凹凸度且土壤含石率較高的溪谷兩者之間。

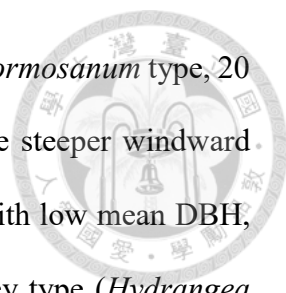
本研究所蒐集之拉拉山森林動態樣區木本植物分布及相關環境狀況，亦可作為未來複查樣區之基線資料，以供未來分析及監測台灣亞熱帶山地雲霧森林動態之所需。

關鍵詞：降趨對應分析、雙向指標種分析、東北季風、亞熱帶山地雲霧森林、植群分類

Abstract

Subtropical montane cloud forest (SMCF) is a peculiar vegetation type, affected by the regular occurrence of dense clouds, which influences plant species due to high air humidity, lower light availability and air temperature, and chronic soil nutrient limitation. To understand the ecological processes behind the SMCF community in Taiwan, we established the Lalashan Forest Dynamics Plot (LFDP) in *Chamaecyparis montane* mixed cloud forest near the saddle between Lalashan and Tamanshan, inside the Chatianshan Nature Reserve, northern Taiwan (24°42' N, 121°26' E). The 1-ha plot was established in July 2019, and in August 2020, we finished the first census of all woody species with a diameter at breast height ≥ 1 cm. Each individual was identified, tagged, mapped, and its diameter at breast height (DBH) was measured. We collected environmental factors related to the topography within each of the 100 10 m \times 10 m subplots and soil properties within selected 25 10 m \times 10 m subplots.

In total, we recorded 5220 individuals belonging to 65 species, 42 genera and 29 families, with a basal area (BA) of 69.1 m²/ha. The forest is dominated by *Chamaecyparis obtusa* var. *formosana* (14% of importance value index, IVI), *Rhododendron formosanum* (14%), *Quercus sessilifolia* (9%), *Trochodendron aralioides* (7%) and *Eurya crenatifolia* (5%), and the cumulative IVI of these five most dominant species reached 49%. We applied modified two-way indicator species analysis (TWINSpan) to classify the vegetation into three vegetation types at subplot-level, and tested differences in environmental conditions between these types by ANOVA. The ridge type (*Daphniphyllum himalayense* subsp. *macropodum*-*Chamaecyparis obtusa* var. *formosana* type, 74 subplots) is the main vegetation type of LFDP, mainly distributed on the wide ridge in the west and middle part of LFDP, with relatively flat topography and soils with lower pH, with higher mean DBH and lower density of individuals. The east-



facing slope type (*Pourthiaea villosa* var. *parvifolia*-*Rhododendron formosanum* type, 20 subplots) is mainly distributed in the eastern part of the plot on the steeper windward slopes facing the northeast monsoon, with soils of higher soil pH, with low mean DBH, higher density of individuals and higher species richness. The valley type (*Hydrangea angustipetala*-*Eurya crenatifolia* type, 6 subplots) is rather rare, distributed in the ephemeral streams in the western part of LFDP, in steeper slopes and concave shapes with high soil rockiness and soil pH, and with the lowest density of individuals.

To uncover the main gradients in species composition, we used detrended correspondence analysis (DCA) with passively projected topographical and soil environmental factors. The results of DCA showed that the vegetation of the plot is structured along two main compositional axes, the first related positively to elevation, soil chemical properties including C/N ratio, available P, Mg, and Zn, and negatively to slope and soil pH, while the second related positively to soil rockiness, and negatively to windwardness, convexity and stabilization factor of decomposition. The main changes in species composition are between steeper, windward slopes with less acid soils, and flatter higher ridges with more acid soils. The second main changes are between more convex types of topography and concave valley types with rockier soils.

This study provides baseline data about the distribution of woody species and relevant environmental conditions in LFDP, which can be used as references for future resurveys, and analyses for monitoring the dynamics of SMCF in Taiwan.

Keywords: detrended correspondence analysis, modified two-way indicator species analysis, northeast monsoon, subtropical montane cloud forest, vegetation classification

Contents



摘要	I
Abstract	III
Contents	V
List of Figures	VI
List of Tables	VII
Abbreviations in this study	VIII
Introduction	1
Materials and Methods	6
<i>Study site</i>	6
<i>Sampling design</i>	8
<i>Species composition</i>	8
<i>Topographical variables</i>	10
<i>Soil properties</i>	11
<i>Statistical analyses</i>	13
Results	15
Discussion	28
Conclusions	32
Authors contributions	33
References	34
Appendices	45
Appendix 1: Synoptic table	45
Appendix 2: The differences between the selected soil chemical properties in DCA	49
Appendix 3: Correlations between environmental variables	50
Appendix 4: Species checklist	51
Appendix 5: Species IVI in LFDP	56
Appendix 6: R code	59

List of Figures



Figure 1. Location of LFDP	7
Figure 2. The 25 selected subplots in LFDP	7
Figure 3. Distribution of the three vegetation types in LFDP.	16
Figure 4. Photographs of the three vegetation types in LFDP.....	18
Figure 5. Boxplots of physiognomic differences between vegetation types	23
Figure 6. Boxplots of environmental differences between vegetation types.....	24
Figure 7. DCA ordination diagram.....	26
Figure S1. Boxplots of differences of the selected soil chemical properties in DCA between vegetation types.....	49
Figure S2. Correlation of significant topographical variables and soil properties variables	50

List of Tables



Table 1. The relationships between environmental factors and DCA axes	27
Table S1. Diagnostic species of the three vegetation types	45
Table S2. Checklist for all woody species	51
Table S3. List of species IVI in whole plot level.....	56

Abbreviations in this study



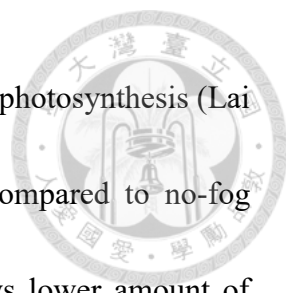
Abbreviation	Original term
ANOVA	analysis of variance
BA	basal area
DBH	diameter at breast height
DCA	detrended correspondence analysis
FDP	forest dynamics plot
ForestGEO	Forest Global Earth Observatory Network
IVI	importance value index
LFDP	Lalashan Forest Dynamics Plot
MCF	montane cloud forest
SMCF	subtropical montane cloud forest
TMCF	tropical montane cloud forest
Tukey's HSD	Tukey's honestly significant difference test
TWINSpan	two-way indicator species analysis



Introduction


Montane cloud forest (MCF) is characterized by the presence of persistent and frequent wind-driven cloud and foggy conditions at ground (tree) level (Hamilton 1995). The distribution of MCF is highly fragmented according to the restriction of persistently foggy zones, making these fragments act like isolated islands which are assumed to promote speciation and endemism (Bruijnzeel et al. 2010; Li et al. 2015). MCF is one of the world's most endangered ecosystems because of their sensitivity to changes in unique ecological conditions (Bruijnzeel et al. 2010). In addition, climate observations show that MCF is suffering from a decreasing trend in ground fog occurrence which is likely related to climate change (Still et al. 1999; Foster 2001; Ponco-Reyes et al. 2012; Hu and Riveros-Iregui 2016).

High fog frequency in MCF is responsible for occurrence of special environmental conditions different from other forest types, including horizontal precipitation, high air humidity, lower light availability, lower air temperature, and chronic nutrient limitation in soil. Horizontal precipitation represents an extra water input, additional to rainfall (vertical precipitation), and is formed when fog condensates on leaf surfaces, a process also known as “fog stripping” (Stadtmüller 1987). High air humidity helps mitigate the temperature differences, but at the same time it makes the transpiration process for plants more difficult, and also makes it easier for epiphylls (including lichens, mosses, algae and



fungi) to grow on and cover the leaves, which may result in reducing photosynthesis (Lai et al. 2006). The presence of fog can reduce 10–15% of light compared to no-fog conditions, causing lower light availability for plants, which allows lower amount of active radiation for photosynthesis, but may lower the effect of photoinhibition and increase photosynthesis efficiency under diffuse light at the same time (Urban et al. 2007; Reinhardt and Smith 2008). When fog occurs, the air temperature is 3–6°C lower than analogous site without fog, making it hard for plants to be threatened by heat stress, but the plants may encounter frost events. Lower air temperature may also lead to relatively low overall heat income for plants, and thus decreases the efficiency of photosynthesis (Lai et al. 2006). Due to very frequent high air/soil humidity and lower air temperature, the decomposition rates in MCFs are slower, causing chronic nutrient limitation in soil (Tanner et al. 1990).

Past studies about MCF were mostly done in tropical montane cloud forest (TMCF), while there are fewer studies done in subtropical montane cloud forest (SMCF), although its biological and conservation value is not less significant (Li et al. 2015). In subtropical eastern Asia, a large proportion of SMCF are evergreen broadleaved forests mixed with coniferous and deciduous broad-leaved trees. The common dominant genera in these mixed forests include the conifers *Chamaecyparis*, *Cryptomeria*, *Cunninghamia*, *Picea*, *Pseudotsuga*, *Taiwania* and *Tsuga*, and the deciduous *Fagus* because of relatively



pronounced seasonality, when frost events may also occur during the winter months (Su 1984; Li et al. 2015). By a common dominance of coniferous species, the SMCF differs from TMCF, which are dominated only by evergreen broad-leaved trees (Bruijnzeel et al. 2010).

Zonal forests in Taiwan can be classified into five vegetative zones based on local climate, which is primarily driven by altitude, and at altitudes around 1500 to 2500 m a.s.l., the montane zone is characterized by frequent ground fog occurrence (Li et al. 2015; Schulz et al. 2017). However, some MCFs in Taiwan atypically distribute in lower altitudes than 1500 m a.s.l. One important reason causing this is the influence of the northeast monsoon, creating local deviations in the altitudinal distribution of ground fog occurrence, which makes MCFs occur at atypically low altitudes in the northeastern part of Taiwan (Lai et al. 2006; Li et al. 2013, 2015; Schulz et al. 2017). The other important reason is the Massenerhebung effect (Quervain et al. 1904), which influences cloud occurrences through the landmass heating effect.

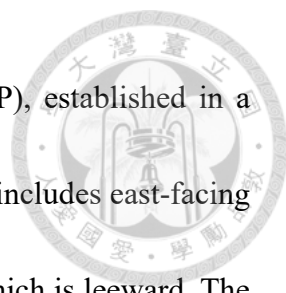
Northeast monsoon strongly influences ground fog occurrences through decreasing the air temperature by increasing the air humidity. Northeast monsoon also influences both compositional and physiognomic structure of the forest; studies done in Nanjenshan and Lanjenchi FDP found that the windward forests influenced by the northeast monsoon has different compositional changes under different wind exposure levels, and also has

denser, shorter and smaller trees than the leeward forests (Chao et al. 2010; Ku et al. 2021, 2022).



MCF in Taiwan include three main subtropical vegetation types, namely *Chamaecyparis* montane mixed cloud forest, *Fagus* montane deciduous broad-leaved cloud forest, and *Quercus* montane evergreen broad-leaved cloud forest, and one tropical vegetation type, namely *Pasania-Elaeocarpus* montane evergreen broad-leaved cloud forest (Li et al. 2013).

Through forest dynamics plot (FDP) studies, we can understand the forest ecosystems and dynamics with detailed and long-term data, which can also monitor the species composition change as a result of the global climate change. However, there are only a few previous FDP studies done in Taiwan and focused on SMCF. These studies include the one done in Yuanyang Lake Long-Term Ecological Research Site (Chou et al. 2000) and two FDPs in Mt. Peitungyen in central Taiwan (Song 1996; Song et al. 2010; Hu and Tzeng 2019), but none of them studied also the effects of monsoon. In contrary, previous FDP studies about the effects of monsoon on forest vegetation in Taiwan contain the studies done in lower elevations, namely one FDP in montane rainforest at Mt. Lopei in northern Taiwan (Lin et al. 2005) and four FDPs in lowland subtropical rainforest at Nanjenshan region in southern Taiwan (Chao et al. 2007, 2010; Ku et al. 2021), from which none belongs to SMCF.



Our study was done in Lalashan Forest Dynamics Plot (LFDP), established in a SMCF in the northern part of Taiwan. The plot is on a flat ridge and includes east-facing slope influenced by the northeast monsoon, and west facing slope which is leeward. The vegetation of LFDP belongs to *Chamaecyparis* montane mixed cloud forest, where coniferous and broad-leaved woody species co-occur, with admixture of deciduous species (Li et al. 2015). We established LFDP in 2019, in order to learn more about the vegetation and the environmental factors influencing a SMCF, and to collect baseline data allowing us to monitor the future vegetation changes which may be caused by climate change. The aims of this study in LFDP are: 1) to describe the woody species composition, and 2) to explore the relationships between the woody species composition and the environmental factors.

Materials and Methods

Study site

We established a one-hectare Lalashan Forest Dynamics Plot (LFDP; 24°42' N, 121°26' E); elevation 1758–1782 m a.s.l.) in July 2019, and finished the first census of woody species in August 2020. LFDP is located on a wide part of the mountain ridge near the saddle between Lalashan (拉拉山) and Tamanshan (塔曼山), inside the Chatianshan Nature Reserve (插天山自然保留區), in northern Taiwan (Fig. 1). The mountain ridge is in the northern part of Xueshan Range (雪山山脈), with orientation of northwest-southeast direction. There are two west-east direction ephemeral streams in the western part of LFDP, and an east-facing slope exposed to the northeast monsoon in the eastern part of LFDP. The vegetation in LFDP belongs to *Chamaecyparis montane* mixed cloud forest (Li et al. 2013), which is dominated by *Chamaecyparis obtusa* var. *formosana* (coniferous species) and *Rhododendron formosanum* (evergreen broadleaf species).



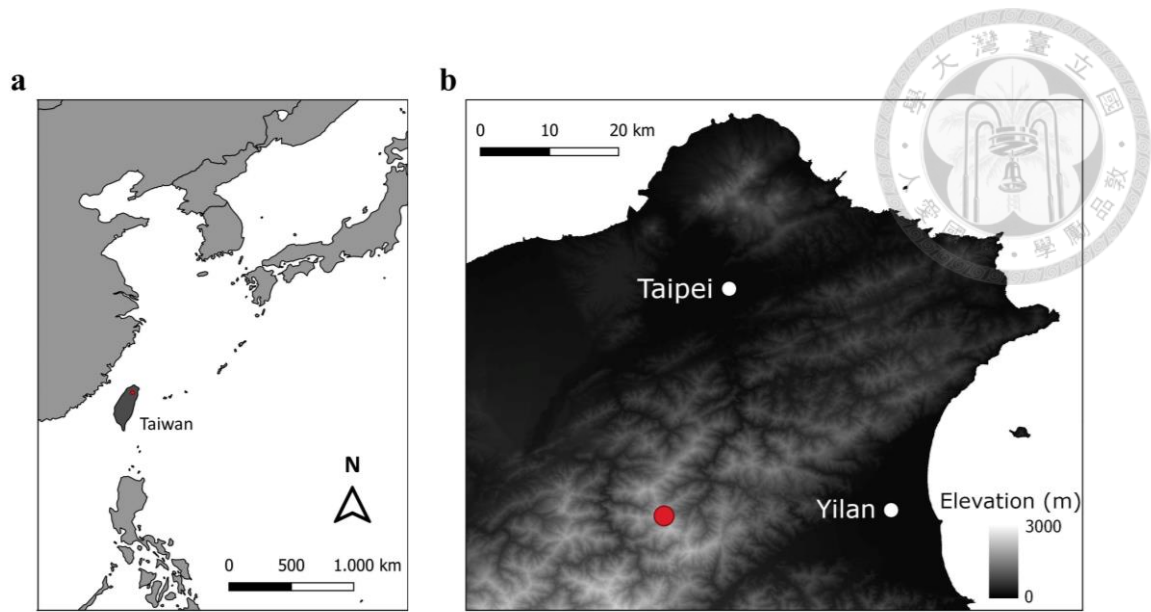


Figure 1. Location of LFDP (red point) in East Asia (a) and in northern Taiwan (b).

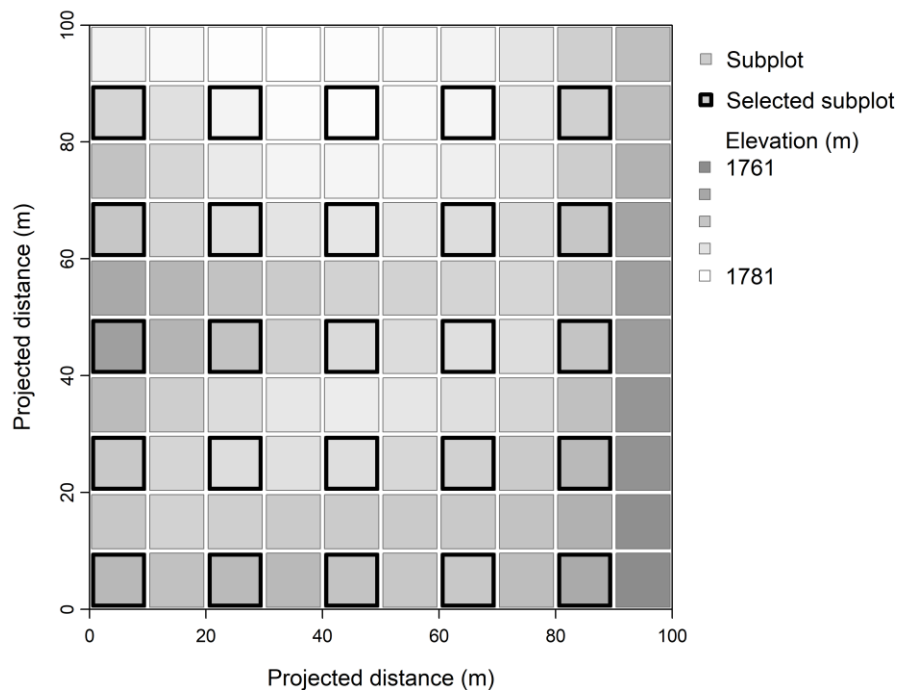


Figure 2. The one-hectare LFDP was subdivided into 100 10 m × 10 m subplots, the soil chemical properties (except soil pH) were only measured in the 25 selected subplots (with thick black boundaries). Subplot-based elevation is shown by gray shading.



Sampling design

The establishment of LFDP and survey of woody species followed the Forest Global Earth Observatory Network (ForestGEO) Tree Census Protocol (Condit 1998). LFDP was established by using a compass with a telescope (Ushikata LS-25, Kantum Ushikata Co. Ltd., Yokohama, Japan) to recalculate the distance according to slope and delineate a projected area of one hectare (100 m × 100 m), which was then subdivided into 100 10 m × 10 m subplots (Fig. 2). The aspect of the main LFDP axis is pointing to the north, and the corners of the subplots were coded with the coordinates, with (0,0) starting from the south-west corner and ending with (10,10) in the north-east corner. The corners of the subplots were marked with PVC poles painted red at the top, and the centers of the subplots were marked with plastic poles painted yellow at the top. The subplot IDs were coded according to the coordinates of their south-west corners.

Species composition

When surveying, we first delineate the boundaries of each subplot with a tape, which facilitates us to determine the trees near the boundaries, only the trees rooted inside the surveyed subplot will be recorded for the subplot. In each subplot, all individuals of woody species (excluding lianas) with diameter at breast height (DBH) ≥ 1 cm were identified, tagged with iron tag with a stamped number, mapped and their DBH measured.



All branches of the same individual with $DBH \geq 1$ cm were also measured and tagged with white plastic tag with a number written by a pencil.

To express species dominance for each subplot, we calculate importance value index (IVI; Curtis 1959) as the sum of relative basal area and relative individual density of each species in the subplot. Basal area (BA) of an individual is calculated as $BA = \pi(DBH/2)^2$, and relative BA is calculated by the sum of BA of all species individuals in the subplot divided by the total BA of all species in the subplot. Relative density is calculated by the numbers of individuals of a species in the subplot divided by the total numbers of individuals of all species in the subplot. IVI for the whole plot was calculated in the same way, with relative BA and relative density calculated from all individuals in LFDP.

For physiognomic variables, we calculated BA and mean DBH for each subplot; BA is the summed BA of all individuals of all species within each subplot, and mean DBH is the mean DBH size of the trees in each subplot. Density is the total number of individuals for each subplot, and species richness is the numbers of species of each subplot. We also calculated total BA for different leaf types of each subplot; the species in LFDP were categorized into three leaf types including conifer, evergreen broadleaf and deciduous broadleaf species, using information from Flora of Taiwan, 2nd edition (Huang & Hsieh 1994–2003) and our field observations.




Topographical variables

The environmental factors related to topography, including elevation, convexity, slope and windwardness, were all derived from the elevation of the poles in corners of subplots.

The elevation of the poles was calculated relatively to the first pole (5,0)'s elevation measured by GPS (GARMIN GPSMAP 64st, USA) and the slope angles between poles recorded while delineating the plot. The elevation of each subplot was calculated as the mean elevation of its four corner poles. The convexity of each subplot was calculated as its elevation minus the mean elevation of its eight-surrounding subplots. For the convexity of the subplots on the margin of the plot (which are not surrounded by eight other subplots), the convexity was calculated as the elevation of the subplot's center pole (additionally measured in the field with Ushikata for all subplots on the margin) minus the elevation of the subplot (calculated as the mean elevation of the four corner poles).

The slope of each subplot was calculated as the mean angular deviation from the horizon of each of the four triangular planes formed by connecting three of the target subplot's corner poles. The elevation, convexity and slope were calculated using "fgeo" packages (version 1.1.4, Lepore et al. 2019) in R programme. The aspect was calculated as the elevation of the midpoints of each subplot's four sides by averaging the elevation of the two corner poles on each side, using the formula $180 - \arctan (f_y / f_x) \cdot (180 / \pi) + 90 (f_x / |f_x|)$, where f_x is the midpoint elevation change from the east side to west side, and f_y is

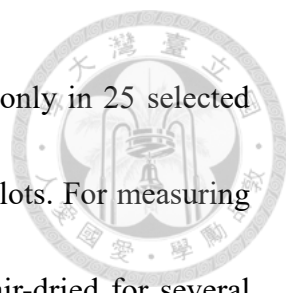


the midpoint elevation change from the north side to south side. The windwardness was calculated by multiplying the slope ($^{\circ}$) and the aspect folded along the E-W axis (by setting $+90^{\circ}$ in the east and -90° in the west), which makes it strongly related to folded aspect, and also has relationship to solar irradiation.

Soil properties

For the collection of soil samples, we first divided one $10\text{ m} \times 10\text{ m}$ subplot into four $5\text{ m} \times 5\text{ m}$ sections, collected the soil at the center of each section from 0–10 cm depth, and mixed the soil collected within the same subplot together.

The soil properties measured in the field included estimated soil rockiness and measured soil depth and were recorded for all 100 subplots. Soil rockiness was estimated as the relative proportion of stones in the soil, respectively at the center of each $5\text{ m} \times 5\text{ m}$ section, and averaged into one value for that subplot. Soil depth was first measured respectively at the center of each $5\text{ m} \times 5\text{ m}$ section with a 30 cm long iron rod (0.6 cm in diameter), the values of soil depth ranged from 0–30 cm, and soil depth deeper than 30 cm was recorded as 30+ cm. We converted the measured values of soil depth into an ordinal scale by replacing 0 cm with 0, 1–5 cm with 1, 6–10 cm with 2, 11–20 cm with 3, 21–30 cm with 4 and 30+ cm with 5, and calculated the median of the values in the same subplot to represent the subplot-based soil depth.



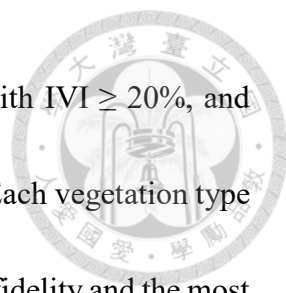
The soil chemical properties were measured in the laboratory only in 25 selected subplots (Fig. 2), except soil pH that was measured for all 100 subplots. For measuring the soil chemical properties, the collected soil samples were first air-dried for several weeks and sieved by 2.0 mm sieve (2.0 mm laboratory test sieve, Endecotts Ltd, England), then measured through the following chemical analyses: soil pH was measured by a glass electrode pH meter (LAQUA F-71, Horiba Ltd., Kyoto, Japan) in the solution of soil sample and deionized water in 1:2 ratio; soil texture (sand, silt and clay) was conducted by hygrometer method (Gee & Bauder 1986); organic C content was acquired by Walkley and Black dichromate method (Nelson & Sommers 1996); total N was determined by Kjeldahl method (Nelson & Sommers 1972); C/N ratio was calculated as organic C divided by total N; exchangeable N, which contained the ammonium-N and nitrate-N, was determined by KCl extraction and steam distillation (Mulvaney 1996); available P was determined by Bray No. 1 method (modified from Burt, 2004) with a spectrometer (UV-1900PC, Macylab Instruments Inc., Shanghai, China); exchangeable cations of K, Ca and Mg were extracted by 1 M ammonium acetate (pH 7) and determined by a flame atomic absorbance spectrophotometer (AAAnalyst 200, PerkinElmer, Inc., Waltham, MA, USA; Burt 2004); and available cations of Fe, Cu, Zn were extracted by 0.1 N HCl and determined by AAAnalyst 200 (Baker & Amacher 1982). The detailed method descriptions of the soil property and chemical analysis are available in Appendix S2 of former lab

member's Master thesis (Lee 2021).

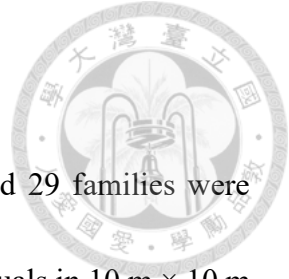
Decomposition rate and stabilization factor were also measured for the 25 subplots, following the protocol proposed by Keuskamp et al. (2013). Green tea and rooibos tea commercial teabags were buried 8 cm deep in the soil in the 25 subplots, then the teabags were collected back for experiments after around 90 days. The teabags were first dried in oven for 48 hours at 70°C, then the remnants of tea were combusted in a muffle oven at 550°C for 16 hours, and the remains were used to calculate decomposition rate and stabilization factor by modified formulas from Keuskamp et al. (2013).

Statistical analyses

With subplot-based IVI data, we classified the forest vegetation at LFDP into three vegetation types by modified two-way indicator species analysis (modified TWINSpan; Hill 1979; Roleček et al. 2009), using R package “twinspanR” (Zelený 2021). In modified TWINSpan, pseudospecies cut levels were set to 0, 2, 5, 10, and 20%, and we used Bray-Curtis distance to measure compositional dissimilarity. For species composition differences between the three vegetation types, we determined diagnostic, dominant and constant species for each vegetation type, using JUICE software (Tichý 2002). Diagnostic species were determined as species with $\Phi \geq 35$ (Φ is a fidelity coefficient phi, Chytrý et al. 2002) in the subplots of a vegetation type, and significant at $P < 0.05$ when tested by



Fisher's exact test. Dominant species were determined as species with $IVI \geq 20\%$, and constant species were determined as species with frequency $\geq 80\%$. Each vegetation type was named by combination of the diagnostic species with the highest fidelity and the most dominant species for this vegetation type. We tested the physiognomic and environmental differences between the three vegetation types by using analysis of variance (ANOVA) and Tukey's honestly significant difference test (Tukey's HSD). Then we visually verified the relationships between the three vegetation types and environmental factors by projecting them onto the ordination diagram of detrended correspondence analysis (DCA; Hill and Gauch 1980), where we also projected the environmental factors that are significantly ($P < 0.05$) related to the first two ordination axes (using `envfit` function in "vegan" package, version 2.5-7, Oksanen et al. 2020). Environmental variables measured within all 100 subplots data were projected onto the DCA ordination when their P-value was lower than 0.05, while environmental variables measured only in the 25 subplots were projected onto the DCA ordination when their P-value was lower than 0.1. All P-values of supplementary variables projected onto DCA were calculated while acknowledging for spatial autocorrelation, using toroidal permutation test (Legendre and Legendre 2012).



Results

A total of 5220 individuals, belonging to 65 species, 42 genera and 29 families were recorded in LFDP, with total BA of $69.1 \text{ m}^2 \text{ ha}^{-1}$. Numbers of individuals in $10 \text{ m} \times 10 \text{ m}$ subplots varied between 11 and 182 with an average of 52.2, and the BA in $10 \text{ m} \times 10 \text{ m}$ subplots varied between $5.5 \text{ m}^2 \text{ ha}^{-1}$ and $191.6 \text{ m}^2 \text{ ha}^{-1}$. The forest in the plot is dominated by *Chamaecyparis obtusa* var. *formosana* (14% of plot-based IVI), *Rhododendron formosanum* (14%), *Quercus sessilifolia* (9%), *Trochodendron aralioides* (7%) and *Eurya crenatifolia* (5%), with the cumulative IVI of these five most dominant species reaching 49%.

We used modified TWINSpan to classify the forest vegetation of LFDP into three vegetation types, and first named them with typical topographical features where they occurred in (Fig. 3): (1) ridge type (Fig. 4a), (2) east-facing slope type (Fig. 4b), and (3) valley type (Fig. 4c). Their compositional, physiognomic and environmental characteristics are described below.

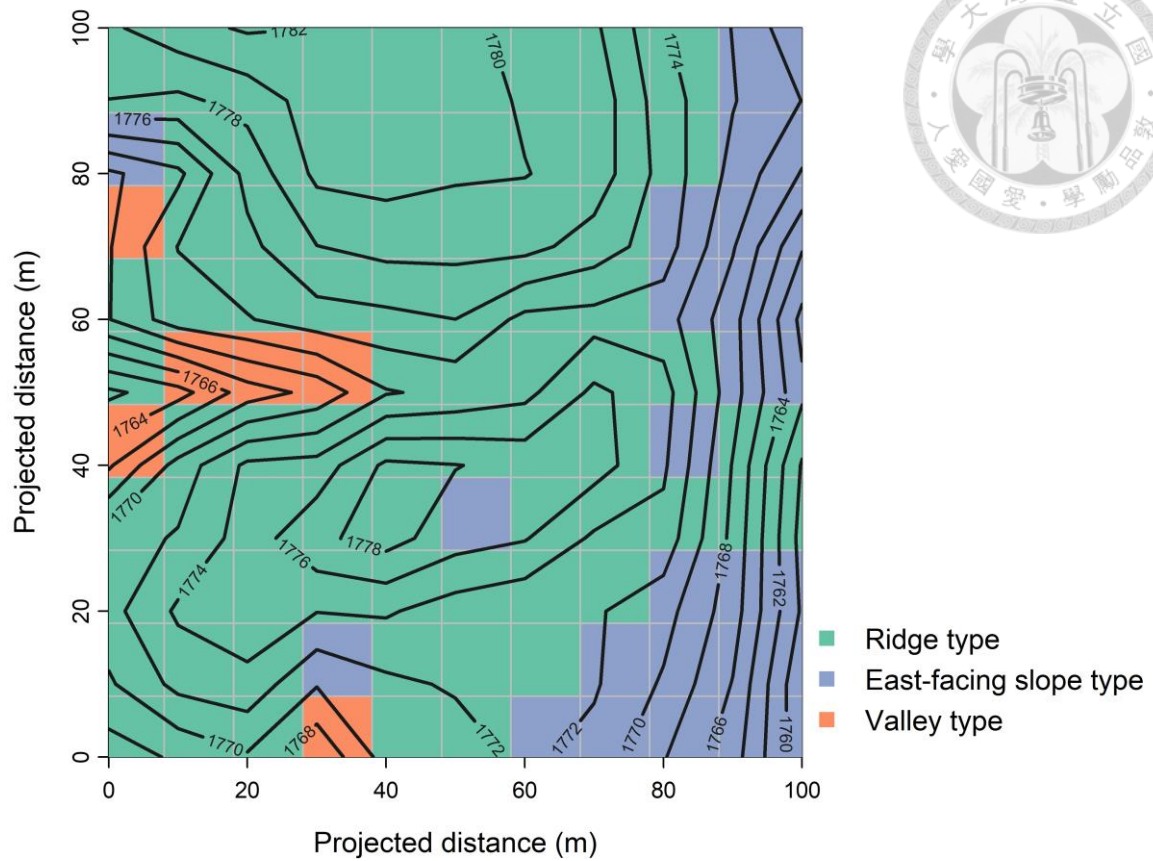
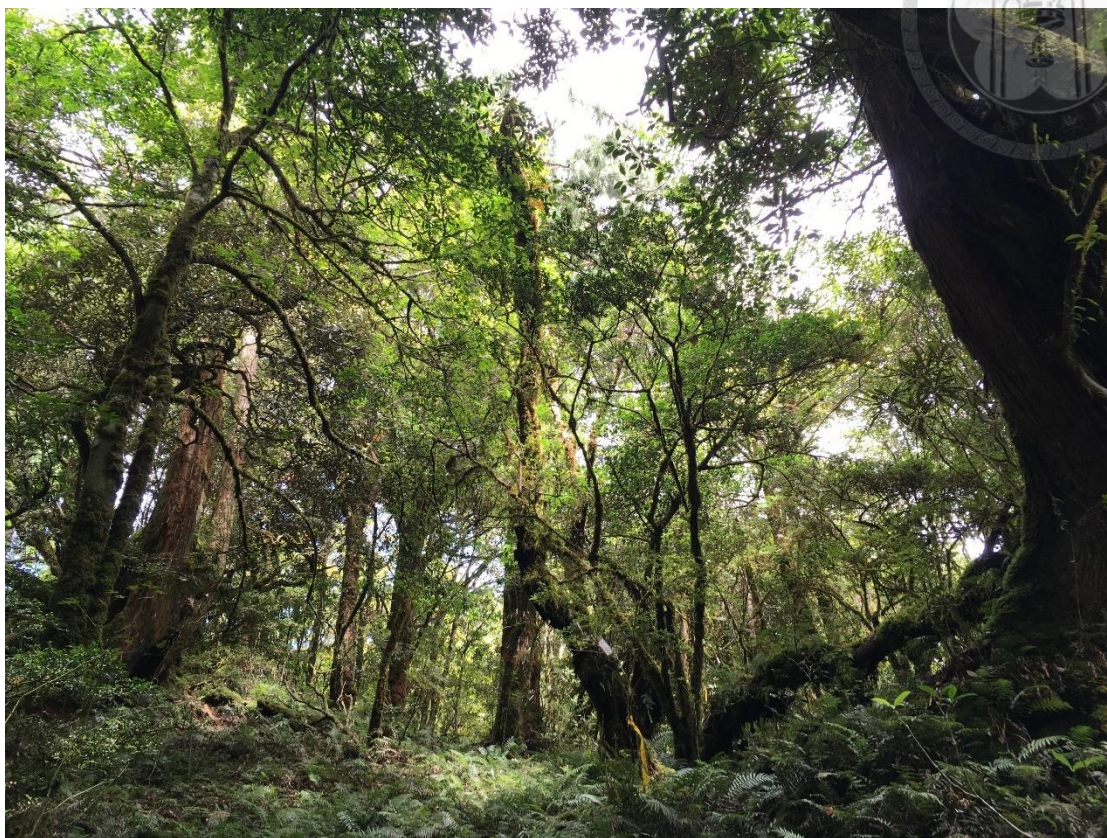


Figure 3. Distribution of the three vegetation types at subplot level in LFDP.



a



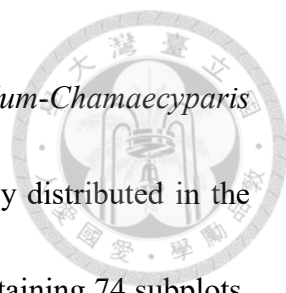
b




c



Figure 4. Photographs of the three vegetation types in LFDP; a. ridge type, b. east-facing slope type, c. valley type.

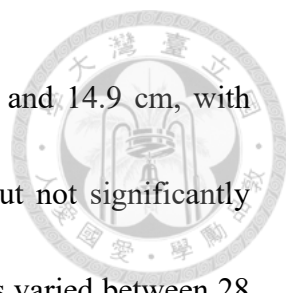


Ridge type (*Daphniphyllum himalayense* subsp. *macropodum*-*Chamaecyparis obtusa* var. *formosana*) is the main vegetation type of LFDP, mostly distributed in the subplots on the wide ridge in the west and middle part of LFDP, containing 74 subplots. Diagnostic species of ridge type include *Daphniphyllum himalayense* subsp. *macropodum* and *Rhododendron formosanum* (listed by decreasing fidelity; Appendix S1: Table S1); dominant species include *Rhododendron formosanum*, *Chamaecyparis obtusa* var. *formosana*, *Quercus sessilifolia*, *Trochodendron aralioides*, *Prunus transarisanensis*, *Quercus longinux*, *Ilex tugitakayamensis*, *Cleyera japonica* and *Acer palmatum* var. *pubescens* (listed by decreasing dominance); and constant species include *Trochodendron aralioides*, *Neolitsea acuminatissima*, *Chamaecyparis obtusa* var. *formosana* and *Cleyera japonica* (listed by decreasing constancy). Ridge type contains 56 species and 3160 individuals in total. For ridge type, BA in 10 m × 10 m subplots varied between 11.3 m² ha⁻¹ and 191.6 m² ha⁻¹, with average of 74.1 m² ha⁻¹; mean DBH in 10 m × 10 m subplots varied between 6.7 cm and 29.5 cm, with average of 15.8 cm, which is significantly higher than east-facing slope type, but not significantly different from valley type (Fig. 5b); density in 10 m × 10 m subplots varied between 11 and 143 individuals, with average of 42.7; species richness in 10 m × 10 m subplots varied between 7 and 25, with average of 14; mean BA of coniferous species is 27.6 m² ha⁻¹, which is significantly higher than east-facing slope type, but not significantly different from valley type (Fig.



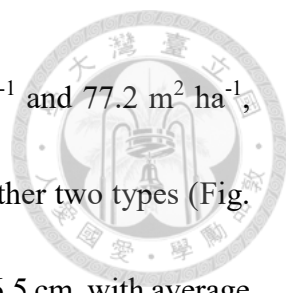
5e); mean BA of evergreen broadleaf species is $42.2 \text{ m}^2 \text{ ha}^{-1}$, which is significantly higher than valley type, but significantly lower than east-facing slope type (Fig. 5f); and mean BA of deciduous broadleaf species $4.3 \text{ m}^2 \text{ ha}^{-1}$, which showed no significant differences among the three vegetation types (Fig. 5g). Ridge type occurs in subplots with higher elevation and convexity; with milder slopes, weaker windwardness, and lower soil rockiness and soil pH (Fig. 6).

East-facing slope type (*Pourthiaea villosa* var. *parvifolia*-*Rhododendron formosanum*) subplots mostly distribute on the east facing windward slopes, containing 20 subplots, diagnostic species of east-facing slope type include *Pourthiaea villosa* var. *parvifolia*, *Eurya glaberrima*, *Viburnum luzonicum*, *Quercus stenophylloides*, *Microtropis fokienensis*, *Osmanthus heterophyllus*, *Tetradium ruticarpum*, *Ilex sugerokii* var. *brevipedunculata*, *Itea parviflora*, *Litsea elongata* var. *mushaensis* and *Skimmia japonica* subsp. *distincte-venulosa* (Appendix S1: Table S1); dominant species include *Rhododendron formosanum*, *Quercus sessilifolia*, *Quercus longinux* and *Neolitsea acuminatissima*; and the constant species include *Symplocos macrostroma*, *Eurya crenatifolia*, *Rhododendron formosanum*, *Neolitsea acuminatissima*, *Quercus sessilifolia*, *Chamaecyparis obtusa* var. *formosana* and *Camellia brevistyla*. East-facing slope type contains 51 species and 1941 individuals in total. For east-facing slope type, BA in $10 \text{ m} \times 10 \text{ m}$ subplots varied between $26.8 \text{ m}^2 \text{ ha}^{-1}$ and $94.8 \text{ m}^2 \text{ ha}^{-1}$, with average of 63.1 m^2



ha⁻¹; mean DBH in 10 m × 10 m subplots varied between 6.3 cm and 14.9 cm, with average of 9.8 cm, which is significantly lower than ridge type, but not significantly different from valley type (Fig. 5b); density in 10 m × 10 m subplots varied between 28 and 184, with average of 97.1, which is significantly higher than the other two types (Fig. 5c); species richness in 10 m × 10 m subplots varied between 14 and 31, with average of 21.9, which is also significantly higher than the other two types (Fig. 5d); mean BA of coniferous species is 3.4 m² ha⁻¹, which is significantly lower than ridge type, but not significantly different from valley type (Fig. 5e); mean BA of evergreen broadleaf species is 56.9 m² ha⁻¹, which is significantly higher than the other two types (Fig. 5f); and mean BA of deciduous broadleaf species is 2.8 m² ha⁻¹. East-facing slope type occurs in subplots with stronger windwardness, steeper slopes, and higher convexity and soil pH; and with lower elevation and soil rockiness (Fig. 6).

Valley type (*Hydrangea angustipetala*-*Eurya crenatifolia* type) subplots mostly distribute on the valley slope in the west part of LFDP, containing 6 subplots, diagnostic species of valley type include *Hydrangea angustipetala* (Appendix S1: Table S1); dominant species include *Quercus sessilifolia*, *Eurya crenatifolia*, *Cleyera japonica*, *Chamaecyparis obtusa* var. *formosana*, *Camellia brevistyla* and *Acer palmatum* var. *pubescens*; and constant species include *Symplocos macrostroma*, *Eurya crenatifolia*, and *Quercus sessilifolia*. Valley type contains 25 species and 119 individuals in total. For



valley type, BA in 10 m × 10 m subplots varied between 5.5 m² ha⁻¹ and 77.2 m² ha⁻¹, with average of 27.4 m² ha⁻¹, which is significantly lower than the other two types (Fig. 5a); mean DBH in 10 m × 10 m subplots varied between 6.1 cm and 26.5 cm, with average of 12.7 cm, which isn't significantly different from either ridge or east-facing slope type (Fig. 5b); density in 10 m × 10 m subplots varied between 14 and 30, with average of 19.8; species richness in 10 m × 10 m subplots varied between 7 and 16, with average of 11.3; mean BA of coniferous species is 12.0 m² ha⁻¹, mean BA of evergreen broadleaf species is 13.9 m² ha⁻¹, which is significantly lower than the other two types (Fig. 5f), and mean IVI of deciduous broadleaf species of valley type is 1.5 m² ha⁻¹. Valley type occurs in subplots with higher soil rockiness and soil pH, and steeper slopes; with lower elevation and convexity, and weaker windwardness; and there are no significant differences in soil depth between different vegetation types (Fig. 6).

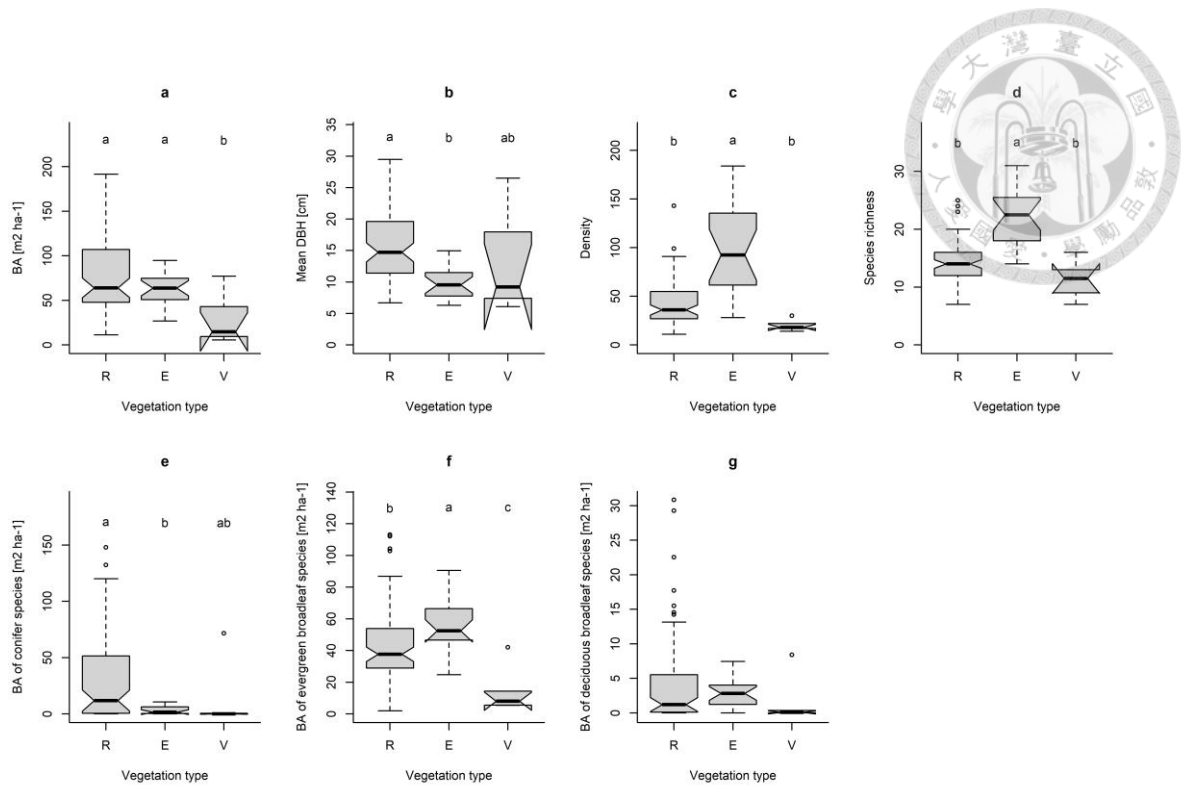


Figure 5. Boxplots showing the subplot-based physiognomic differences between the three vegetation types; a. BA, b. mean DBH, c. density, d. species richness, e. BA of conifer species, f. BA of evergreen broadleaf species, g. BA of deciduous broadleaf species. All differences between vegetation types, except for g, are significant ($P < 0.05$) through ANOVA test. R: ridge type, E: east-facing slope type, V: valley type.

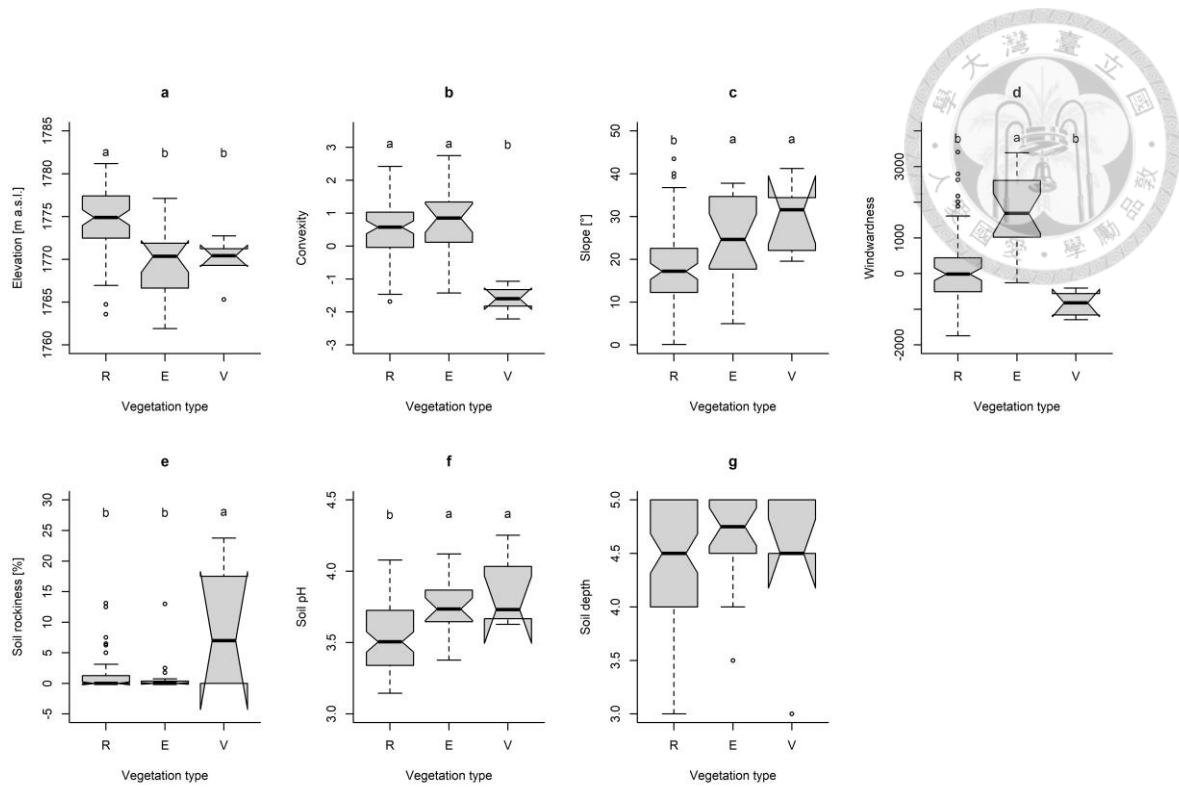
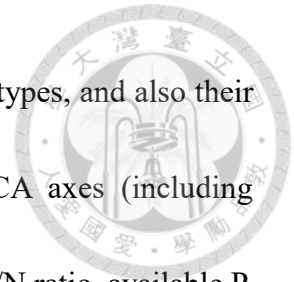


Figure 6. Boxplots showing the differences of different environmental factors (containing 100 subplots data) between the three vegetation types; a. elevation, b. convexity, c. slope, d. windwardness, e. soil rockiness, f. soil pH, g. soil depth. All differences between the vegetation types, except for g, are significant through ANOVA test. R: ridge type, E: east-facing slope type, V: valley type.

The result of DCA shows the relationships between vegetation types, and also their relationships to environmental factors significantly related to DCA axes (including elevation, convexity, slope, windwardness, soil rockiness, soil pH, C/N ratio, available P, Mg, Zn and stabilization factor; Fig. 7; Table 1) The eigenvalue of the first DCA axis is 0.254, and the eigenvalue of the second DCA axis is 0.185.



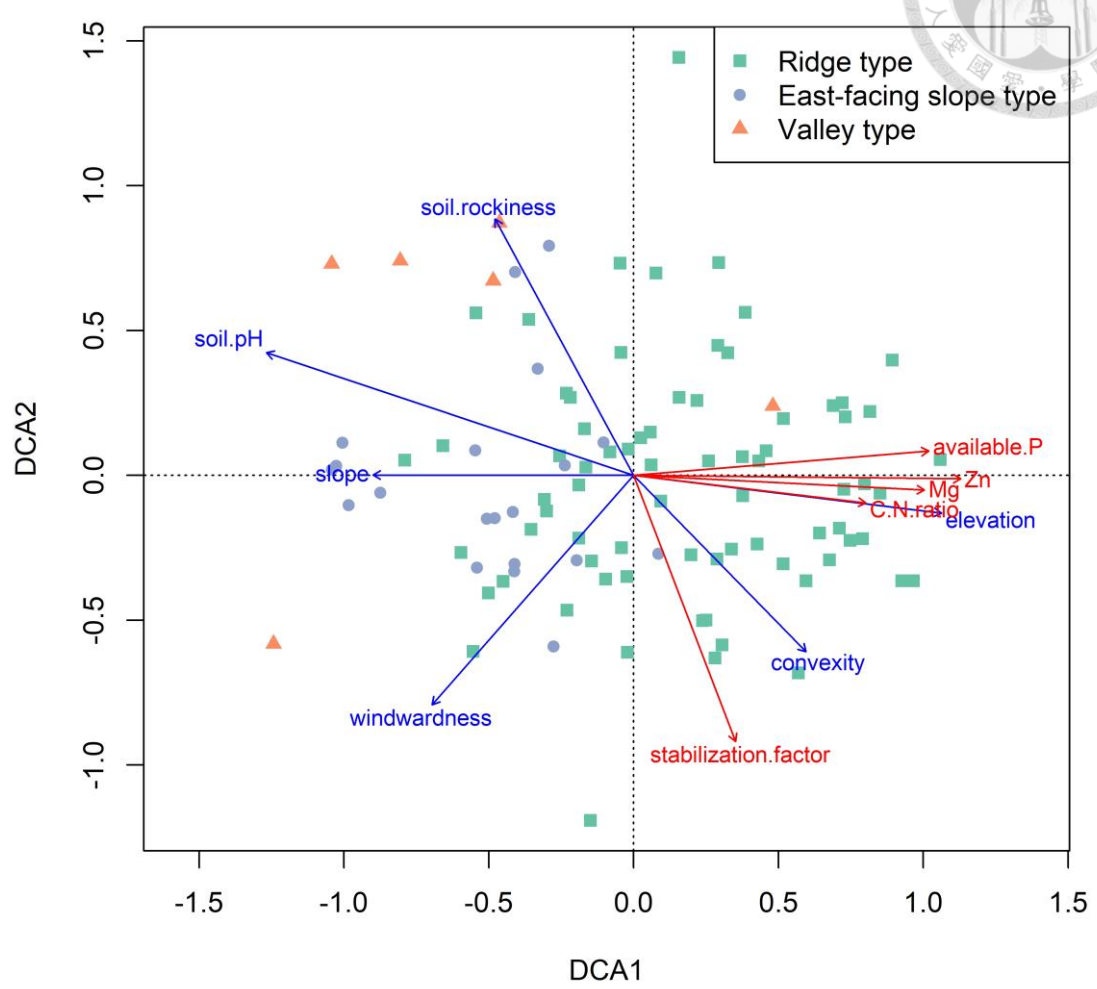


Figure 7. DCA ordination diagram showing the relationships of the three vegetation types and environmental factors; significant environmental factors were projected onto the DCA ordination, the ones projected in blue were measured for 100 subplots data (significant when P-value < 0.05), and the ones projected in red were only measured for 25 subplots data (significant when P-value < 0.1).

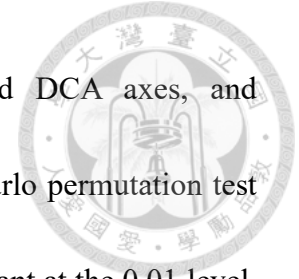


Table 1. The relationships between environmental factors and DCA axes, and significance level of environmental factors calculated by Monte Carlo permutation test using toroidal shift (‘***’ significant at the 0.001 level, ‘**’ significant at the 0.01 level, ‘*’ significant at the 0.05 level, ‘.’ significant at the 0.1 level).

	Axis 1	Axis 2	r ²	Pr (>r)	Number of subplots
Elevation	0.992	-0.122	0.172	0.028 *	100
Convexity	0.699	-0.715	0.109	0.015 *	100
Slope	-1.000	0.001	0.122	0.045 *	100
Windwardness	-0.660	-0.751	0.167	0.043 *	100
Soil depth	0.989	-0.151	0.003	0.843	100
Soil rockiness	-0.475	0.880	0.152	0.003 **	100
Soil pH	-0.948	0.317	0.269	0.003 **	100
Sand	0.703	0.711	0.102	0.450	25
Silt	-0.902	-0.432	0.111	0.440	25
Clay	-0.328	-0.945	0.055	0.540	25
C	0.999	-0.050	0.145	0.140	25
tN	1.000	-0.007	0.110	0.240	25
C/N ratio	0.999	-0.050	0.225	0.060 .	25
eN	0.966	0.260	0.204	0.190	25
available P	0.997	0.082	0.309	0.040 *	25
K	0.999	-0.040	0.093	0.390	25
Ca	0.780	0.626	0.136	0.180	25
Mg	0.999	-0.050	0.298	0.010 **	25
Fe	0.004	-1.000	0.044	0.750	25
Cu	-0.939	-0.343	0.067	0.320	25
Zn	1.000	-0.010	0.377	0.010 **	25
Stabilization factor	0.399	-0.917	0.249	0.030 *	25
Decomposition rate	-0.901	-0.433	0.144	0.140	25




Discussion

In this study, we established the one-hectare Lalashan Forest Dynamics Plot in the subtropical montane cloud forest, surveyed its woody species composition, and explored the relationship of vegetation to environment by classifying the forest vegetation into three types (ridge, east-facing slope, and valley), and by calculating unconstrained ordination of species composition combined with environmental factors.

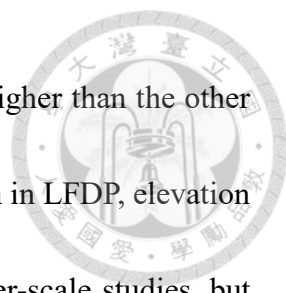
In the east-facing slope vegetation type, both density and species richness are significantly higher than the ridge and valley vegetation types. Windwardness is also significantly higher in east-facing slope type than the other two vegetation types. Since windwardness indicates the degree of facing towards northeast monsoon at subplot level, it reflects the wind conditions influenced by topography at finer scales. It is often observed that forests become denser and shorter as a response to chronic wind (Lawton 1982), which may be the reason why the east-facing slope type forest in LFDP has significantly higher density than the other two vegetation types. Similar dense stands can also be found in other windward-type forests in Taiwan, including the forest dynamics plots at Mt. Lopei (Lin et al. 2005) and Lanjenchi (Chao et al. 2007, 2010; Ku et al. 2021), which are also influenced by northeast monsoon.

In LFDP, the subplot-level species richness in east-facing slope vegetation type is significantly higher than the other two vegetation types. This corresponds to the findings



in forest dynamics plots at Mt. Lopei (Lin et al. 2005) and Lanjenchi (Chao et al. 2007, 2010; Ku et al. 2021), where windward vegetation types also have higher species richness than other forest types recognized in these plots. In our study, the numbers of diagnostic species of east-facing slope vegetation type are higher than those of ridge and valley types, and the fidelity of diagnostic species for east-facing slope type are also higher than the other two types. The study done by Ku et al. (2021) in Lanjenchi FDP also mentioned that there are higher numbers of diagnostic species for windward type forest, and a high proportion of rare species preferring windward habitats, which highlights the unique environmental role of wind to create higher species diversity.

Although east-facing slope type forest has significantly higher density of individuals than the other two types, the averaged BA of east-facing slope type isn't significantly higher than ridge type (but averaged BA of east-facing slope and ridge type are both significantly higher than valley type). Since on the one hand, ridge type forest has significantly higher mean DBH and BA of conifer species than east-facing slope type forest, which mainly attributes to large individuals of *Chamaecyparis obtusa* var. *formosana*; and on the other hand, forest of east-facing slope type are mostly composed of trees with small DBH and multiple stems, which seems to be adapted to the stressful wind conditions caused by northeast monsoon (Fajardo and McIntire 2010; McIntire and Fajardo 2011; Ku et al. 2021).



In the ridge type forest of LFDP, its elevation is significantly higher than the other two vegetation types; however, since the elevation range is only 20 m in LFDP, elevation cannot be seen as proxy of temperature and precipitation as in larger-scale studies, but instead it is more related to convexity or slope in LFDP. In ridge type, both its slope and soil pH are significantly lower than the other two vegetation types. On the one hand, since the ridge type has high dominance of conifer trees on the wide flat ridge, it is likely to accumulate litter of conifer trees that are hard to decompose, which increases the C/N ratio and lowers the soil pH in the soil in such subplots (Finzi et al. 1998; Satti et al. 2003; Hobbie et al. 2006). On the other hand, since ridge type subplots were mostly distributed on the flat ridge, cations in the soil are easy to leach out, which may also lower the soil pH on the ridge. In the boxplots of selected soil chemical properties, ridge type subplots contain higher C/N ratio than the other two vegetation types, although the differences in C/N ratio among vegetation types are not significant (Appendix 2: Fig. S1).

C/N ratio, available P, Mg and Zn are significantly and positively related to each other, and significantly and negatively related to soil pH in LFDP (Appendix 3: Fig. S2). In typical conditions, P is less available in soils with lower pH due to high level of aluminum and iron cations, which form strong combinations with P and restrict its solubility (SanClements 2010). However, in LFDP, available P has negative correlation with soil pH, which we speculate is the result of the slow litter decomposition (which


accumulates the organic acid and lowers the soil pH instead), but not from the weathering process of the soil, and may thus be unavailable for plants.



Mg is often missing in acid soils (soil pH < 5.5) which exhibit higher leaching rates (Schachtschabel 1954; von Uexküll and Mutert 1995; Gransee and Führs 2013), i.e. results from study in Lanjenchi FDP showed that windward habitat exhibited higher Mg that resulted from strong leaching, and flat leeward habitat exhibited relatively low Mg that resulted from relatively low leaching rate (Hsieh et al. 1992). In LFDP, however, Mg also has negative correlation with soil pH, which we speculate may have similar explanation as for available P in LFDP, where higher Mg in subplots with higher elevation and lower slope may attribute to the accumulated litter, since Mg is held on the surface of organic matter particles, and won't readily leach from soils.


Zn is greatly influenced by soil acidity and is often lower in low soil pH, where mineralization is limited (Bergkvist et al. 1989; Rigueiro-Rodríguez et al. 2012). The study by Tsui et al. (2004) also showed that, in the upper 5 cm soil, Zn is positively correlated with soil pH, and negatively correlated with slope. However, Zn is also negatively correlated to soil pH in LFDP, which we speculate that it might be similar to the findings in available P and Mg in LFDP, that the higher amount of Zn is resulted from the accumulation of organic matter, where soil pH was lowered according to organic acid.

Conclusions



To understand the woody species composition of subtropical montane cloud forest (SMCF) and explore its relationship to environment, we established the one-hectare Lalashan Forest Dynamics Plot (LFDP) in the SMCF in Lalashan region. After surveying the woody species composition in LFDP, we classified by modified TWINSpan the forest vegetation into three types: ridge, east-facing slope and valley type. These vegetation types are different in compositional, physiognomic and environmental characteristics. Through the results from DCA, we knew that among the environmental factors we collected in LFDP, elevation, convexity, slope, windwardness, soil rockiness, soil pH, C/N ratio, available P, Mg, Zn and stabilization factor are significantly related to the woody species composition in LFDP. Among these environmental factors, windwardness is the main factor that distinguished east-facing slope type from the other two types. Ridge type is distinguished through milder slopes and lower soil pH, and valley type is distinguished through lower convexity and higher soil rockiness. This study also provides baseline data about the distribution of woody species in LFDP and relevant environmental conditions, and will be used as references for future resurveys.

Authors contributions



The original idea was suggested by Dr. David Zelený and Dr. Ching-Feng Li. Ting Chen, lab members from the Vegetation Ecology Lab directed by Dr. David Zelený and volunteers established LFDP and collected the woody species composition data and environmental factors data in LFDP. Ting Chen, Yi-Nuo Lee, and Kun-Sung Wu maintained the woody species composition data and environmental factors data in LFDP. Ting Chen, lab members from the Vegetation Ecology Lab directed by Dr. David Zelený and lab members from Soil Survey and Remediation Lab directed by Dr. Zeng-Yi Hsu analyzed the soil samples. The tea bag decomposition experiment was conducted by Po-Yu Lin from the Vegetation Ecology Lab. Ting Chen conducted the analyses of woody species composition and environmental factors data for the results, prepared the interpretation of results and discussion. Dr. David Zelený contributed to the interpretations of the results and discussion.



References

- Baker, D.E. and Amacher, M.C. (1982) Nickel, copper, zinc, and cadmium. In: Page, A.L. et al. (Eds), *Methods of Soil Analysis, Part 2: Chemical and Microbiological Properties*, 2nd ed., Madison, WI: Soil Science Society of America, Inc. and American Society of Agronomy, Inc., pp. 323–336.
- Bergkvist, B., Folkesson, L., and Berggren, D. (1989) Fluxes of Cu, Zn, Pb, Cd, Cr, and Ni in temperate forest ecosystems. *Water, Air, and Soil Pollution*, 47, 217–286.
<https://doi.org/10.1007/BF00279328>
- Bruijnzeel, L.A., Scatena, F.N. and Hamilton, L.S. (Eds) (2010) *Tropical montane cloud forests: science for conservation and management*, Cambridge: Cambridge University Press.
- Burt, R. (Ed) (2004) *Soil Survey Laboratory Manual, Soil Survey Investigations Report, No. 42, Version 4.0*. Washington, DC: Natural Resource Conservation Service, US Department of Agriculture.
- Chao, W.-C., Chao, K.-J., Song, G.-Z. M. and Hsieh, C.-F. (2007) Species composition and structure of the lowland subtropical rainforest at Lanjenchi, southern Taiwan. *Taiwania*, 52, 253–269. [http://dx.doi.org/10.6165/tai.2007.52\(3\).253](http://dx.doi.org/10.6165/tai.2007.52(3).253)
- Chao, W.-C., Song, G.-Z.M., Chao, K.-J., Liao, C.-C., Fan, S.-W., Wu, S.-H., Hsieh, T.-H. and Hsieh, C.-F. (2010) Lowland rainforests in southern Taiwan and Lanyu, at



the northern border of Paleotropics and under the influence of monsoon wind.

Plant Ecology, 210, 1–17. <http://dx.doi.org/10.1007/s11258-009-9694-0>

Chou, C.-H., Chen, T.-Y., Liao, C.-C. and Peng, C.-I. (2000) Long-term Ecological Research in the Yuanyang Lake Forest Ecosystem I. Vegetation Composition and Analysis. *Botanical Bulletin of Academia Sinica*, 41, 61–72. <http://dx.doi.org/10.7016/BBAS.200001.0061>

Chytrý, M., Tichý, L., Holt, J. and Botta-Dukát, Z. (2002) Determination of diagnostic species with statistical fidelity measures. *Journal of Vegetation Science*, 13, 79–90. <https://doi.org/10.1111/j.1654-1103.2002.tb02025.x>

Condit, R. (1998) *Tropical forest census plots: methods and results from Barro Colorado Island, Panama and a comparison with other plots*. Texas: Springer.

Curtis, J.T. (Ed) (1959) *The vegetation of Wisconsin: an ordination of plant communities*. Madison, WI: University of Wisconsin Press.

Fajardo, A. and McIntire, E.J. (2010) Merged trees in second-growth, fire-origin forests in Patagonia, Chile: positive spatial association patterns and their ecological implications. *American Journal of Botany*, 97, 1424–1430. <http://dx.doi.org/10.3732/ajb1000054>

Finzi, A.C., Breemen, N.V. and Canham, C.D. (1998) Canopy tree-soil interactions within temperate forests: species effects on soil carbon and nitrogen. *Ecological*



Applications, 8, 440–446. [https://doi.org/10.1890/1051-0761\(1998\)008\[0440:CTSIWT\]2.0.CO;2](https://doi.org/10.1890/1051-0761(1998)008[0440:CTSIWT]2.0.CO;2)

Foster, P. (2001) The potential negative impacts of global climate change on tropical montane cloud forests. *Earth-Science Reviews*, 55, 73–106. [https://doi.org/10.1016/S0012-8252\(01\)00056-3](https://doi.org/10.1016/S0012-8252(01)00056-3)

Gee, G.W. and Bauder, J.W. (1986) Particle-size analysis. In: Klute, A. (Ed), *Methods of Soil Analysis, Part 1: Physical and Mineralogical Methods*, 2nd edition. Madison, WI: Soil Science Society of America, Inc. and American Society of Agronomy, Inc., pp. 383–411.

Gransee, A. and Führs, H. (2013) Magnesium mobility in soils as a challenge for soil and plant analysis, magnesium fertilization and root uptake under adverse growth conditions. *Plant and Soil*, 368, 5–21. <https://doi.org/10.1007/s11104-012-1567-y>

Hamilton, L.S., Juvik, J.O. and Scatena, F.N. (Eds) (1995) *Tropical Montane Cloud Forests*. New York: Springer-Verlag.

Hill, M.O. (1979) TWINSPAN: A fortran program for arranging multivariate data in an ordered two-way table by classification of the individuals and attributes. Ithaca, New York: Ecology and Systematics, Cornell University.

Hill, M.O. and Gauch, H.G. (1980). Detrended correspondence analysis: an improved ordination technique. *Vegetatio*, 42, 47–58. <https://doi.org/10.1007/BF00048870>

Hobbie, S.E., Reich, P.B., Oleksyn, J., Ogdahl, M., Zytkowskiak, R., Hale, C. and Karolewski, P. (2006) Tree species effects on decomposition and forest floor dynamics in a common garden. *Ecology*, 87, 2288–2297. [https://doi.org/10.1890/0012-9658\(2006\)87\[2288:TSEODA\]2.0.CO;2](https://doi.org/10.1890/0012-9658(2006)87[2288:TSEODA]2.0.CO;2)

Hsieh, C.-F., Chen, Z.-S., Sun, I.-F., Hsieh, T.-H., Zheng, Y.-B., Wang, K.-H., Su, M.-H. and Jiang, F.-Y. (1992) The subtropical rain forest in Nanjenshan Area, Kenting National Park (Report No. RES085) (Chinese). Taiwan: Kenting National Park, Construction and Planning Agency, Ministry of the Interior.

Hu, J. and Riveros-Iregui, D.A. (2016) Life in the clouds: are tropical montane cloud forests responding to changes in climate? *Oecologia*, 180, 1061–1073. <https://doi.org/10.1007/s00442-015-3533-x>

Hu, Y.-W. and Tzeng, H.-Y. (2019) Microhabitat types and tree species composition in an evergreen broadleaf forest at Mt. Peitungyen (Chinese). *Taiwan Journal of Forest Science*, 34, 13–27.

Huang, T.-C. and Hsieh, C.-F. (1994–2003). Flora of Taiwan, vol. I–IV, 2nd ed., National Taiwan University, Taipei.



Keuskamp, J.A., Dingemans, B.J.J., Lehtinen, T., Sameel, J.M. and Hefting, M.M. (2013)

Tea Bag Index: a novel approach to collect uniform decomposition data across ecosystems. *Methods in Ecology and Evolution*, 4, 1070–1075.

<https://doi.org/10.1111/2041-210X.12097>

Ku, C.-C., Song, G.-Z. M., Chao, K.-J. and Chao, W.-C. (2021) Species-habitat

associations of tree species under the northeast monsoon wind-affect tropical forest at Lanjenchi Forest Dynamics Plot, Taiwan. *Taiwania*, 66, 39–47.

<http://dx.doi.org/10.6165/tai.2021.66.39>

Ku, C.-C., Chao, K.-J., Song, G.-Z.M., Lin, H.-Y., Fan, S.-W. and Chao, W.-C. (2022)

How the strength of monsoon winds shape forest dynamics. *Diversity*, 14, 169.

<https://doi.org/10.3390/d14030169>

Lai, I.-L., Chang, S.-C., Lin, P.-H., Chou, C.-H. and Wu, J.-T. (2006) Climatic

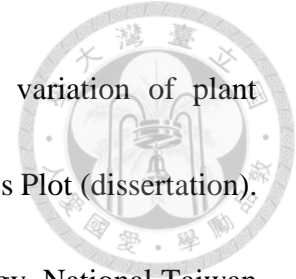
characteristics of the subtropical mountainous cloud forest at Yuanyang Lake long-term ecological research site, Taiwan. *Taiwania*, 51, 317–329.

[http://dx.doi.org/10.6165/tai.2006.51\(4\).317](http://dx.doi.org/10.6165/tai.2006.51(4).317)

Lawton, R.O. (1982) Wind stress and elfin stature in a montane rain forest tree: an

adaptive explanation. *American Journal of Botany*, 69, 1224–1230.

<https://doi.org/10.2307/2442746>



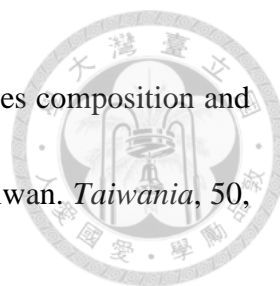
Lee, Y.-N. (2021) Importance of interspecific and intraspecific variation of plant functional traits: a case study in the Lalashan Forest Dynamics Plot (dissertation). Taipei, Taiwan: Institute of Ecology and Evolutionary Biology, National Taiwan University. <https://doi.org/10.6342/NTU202104070>

Legendre, P. and Legendre, L. (2012) *Numerical Ecology, Chapter 1.1: Spatial structure, spatial dependence, spatial correlation*, 3rd ed., Oxford: Elsevier, pp. 8–21.

Lepore, M., Arellano, G., Condit, R., Davis, S., Detto, M., Gonzale-Akre, E. et al. (2019) *Fgeo: analyze forest diversity and dynamics*. Available at: <https://cran.r-project.org/web/packages/fgeo/index.html> [Accessed 30 July 2021]

Li, C.-F., Chytrý, M., Zelený, D., Chen, M.-Y., Chen, T.-Y., Chiou, C.-R., Hsia, Y.-J., Liu, H.-Y., Yang, S.-Z., Yeh, C.-L., Wang, J.-C., Yu, C.-F., Lai, Y.-J., Chao, W.-C. and Hsieh, C.-F. (2013) Classification of Taiwan forest vegetation. *Applied Vegetation Science*, 16, 698–719. <https://doi.org/10.1111/avsc.12025>

Li, C.-F., Zelený, D., Chytrý, M., Chen, M.-Y., Chen, T.-Y., Chiou, C.-R., Hsia, Y.-J., Liu, H.-Y., Yang, S.-Z., Yeh, C.-L., Wang, J.-C., Yu, C.-F., Lai, Y.-J., Guo, K. and Hsieh, C.-F. (2015) Chamaecyparis montane cloud forest in Taiwan: ecology and vegetation classification. *Ecological Research*, 30, 771–791. <https://doi.org/10.1007/s11284-015-1284-0>



Lin, H.-Y., Yang, K.-C., Hsieh, T.-H. and Hsieh, C.-F. (2005) Species composition and structure of a montane rainforest of Mt. Lopei in northern Taiwan. *Taiwania*, 50, 234–249. [http://dx.doi.org/10.6165/tai.2005.50\(3\).234](http://dx.doi.org/10.6165/tai.2005.50(3).234)

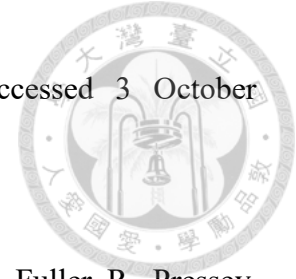
McIntire, E.J. and Fajardo, A. (2011) Facilitation within species: A possible origin of group-selected superorganisms. *The American Naturalist*, 178, 88–97. <http://dx.doi.org/10.5061/dryad.8869>

Mulvaney, R.L. (1996) Nitrogen—inorganic forms. In: Sparks, D.L. et al. (Eds), *Methods of Soil Analysis, Part 3: Chemical Methods*. Madison, WI: Soil Science Society of America, Inc. and American Society of Agronomy, Inc., pp. 1123–1184.

Nelson, D.W. and Sommers, L.E. (1972) A simple digestion procedure for estimation of total nitrogen in soils and sediments. *Journal of Environmental Quality*, 1, 423–425.

Nelson, D.W. and Sommers, L.E. (1996) Total carbon, organic carbon and organic matter. In: Sparks, D.L. et al. (Eds), *Methods of Soil Analysis, Part 3: Chemical Methods*. Madison, WI: Soil Science Society of America, Inc. and American Society of Agronomy, Inc., pp. 961–1010.

Oksanen, J., Blanchet, F.G., Friendly, M., Kindt, R., Legendre, P., McGlinn, D. et al. (2020) *Vegan: community ecology package*. Version 2.5-7. Available at



<https://cran.rproject.org/web/packages/vegan/index.html> [Accessed 3 October 2021]

Ponco-Reyes, R., Reynoso-Rosales, V.H., Watson, J., VanDerWal, J., Fuller, R., Pressey, R. and Possingham, H. (2012) Vulnerability of cloud forest reserves in Mexico to climate change. *Nature Climate Change*, 2, 448–452.
<https://doi.org/10.1038/nclimate1453>

Quervain A.D. (1904) Die Hebung der atmosphärischen Isothermen in der Schweizer Alpen und ihre Beziehung zu deren Höhengrenzen. *Gerlands Beiträge zur Geophysik*, 6, 481–533.

Reinhardt, K. and Smith, W.K. (2008) Impacts of cloud immersion on microclimate, photosynthesis and water relations of *Abies fraseri* (Pursh.) Poiret in a temperate mountain cloud forest. *Oecologia*, 158, 229–238.
<http://dx.doi.org/10.1007/s00442-008-1128-5>

Rigueiro-Rodríguez, A., Mosquera-Losada, M.R., and Ferreiro-Domínguez, N. (2012) Pasture and soil zinc evolution in forest and agriculture soils of Northwest Spain three years after fertilisation with sewage sludge. *Agriculture, Ecosystems & Environment*, 150, 111–120. <https://doi.org/10.1016/j.agee.2012.01.018>

Roleček, J., Tichý, L., Zelený, D. and Chytrý, M. (2009) Modified TWINSpan classification in which the hierarchy respects cluster heterogeneity. *Journal of*



Vegetation Science, 20, 596–602. <https://doi.org/10.1111/j.1654-1103.2009.01062.x>

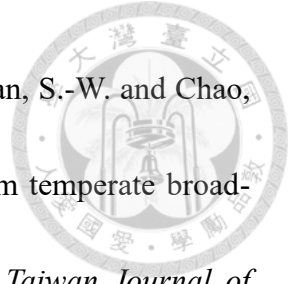
SanClements, M.D., Fernandez, I.J., and Norton, S.A. (2010) Phosphorus in soils of temperate forests: linkages to acidity and aluminum. *Soil Science Society of America Journal*, 74, 2175-2186. <https://doi.org/10.2136/sssaj2009.0267>

Satti, P., Mazzarino, M.J., Gobbi, M., Funes, F., Roselli, L. and Fernandez, H. (2003) Soil N dynamics in relation to leaf litter quality and soil fertility in north-western Patagonia forests. *Journal of Ecology*, 91, 173–181. <https://doi.org/10.1046/j.1365-2745.2003.00756.x>

Schachtschabel, P. (1954) Das pflanzenverfügbare Magnesium des Bodens und seine Bestimmung. *Journal of Plant Nutrition Soil Science*, 67, 9–23.

Schulz, H.M., Li, C.-F., Thies, B., Chang, S.-C. and Bendix, J. (2017) Mapping the montane cloud forest of Taiwan using 12 year MODIS-derived ground fog frequency data. *PLOS ONE*, 12, 1–17. <https://doi.org/10.1371/journal.pone.0172663>

Song, G.-Z. (1996) The composition and distribution type in a warm temperate broad-leaved evergreen forest at Mt Peitungyen, central Taiwan (dissertation) (Chinese). Taipei, Taiwan: Institute of Plant Biology, National Taiwan University.



- Song, G.-Z. M., Yang, K.-C., Hou, C.-H., Lin, J.-K., Hsieh, C.-F., Fan, S.-W. and Chao, W.-C., 2010. Tree population dynamics over 12 yr in a warm temperate broad-leaved evergreen forest at Mt Peitungyen, central Taiwan. *Taiwan Journal of Forest Science*, 25, 17–27. <http://dx.doi.org/10.7075%2fTJFS.201003.0001>
- Stadtmüller, T. (1987) *Cloud forest in the humid tropics*. Costa Rica: The United Nations University.
- Still, C., Foster, P.N. and Schneider, S.H. (1999) Simulating the effects of climate change on tropical montane cloud forests. *Nature*, 398, 608–610. <https://doi.org/10.1038/19293>
- Su, H.-J. (1984) Studies on the climate and vegetation types of the natural forests in Taiwan (II)—Altitudinal vegetation zones in relation to temperature gradient. *Quarterly Journal of Chinese Forestry*, 17, 57–73.
- Tanner, E.V.J., Kapos, V., Freskos S. and Theobald, A.M. (1990) Nitrogen and phosphorus fertilization of Jamaican montane forest trees. *Journal of Tropical Ecology*, 6, 231–238. <http://dx.doi.org/10.1017/S0266467400004375>
- Tichý, L. (2002) JUICE, software for vegetation science. *Journal of Vegetation Science*, 13, 451–453. <https://doi.org/10.1111/j.1654-1103.2002.tb02069.x>

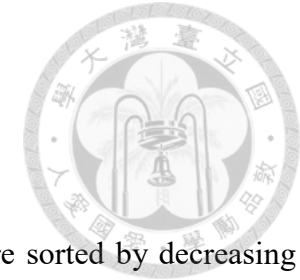
Tsui, C.-C., Chen, Z.-S., and Hsieh, C.-F. (2004) Relationships between soil properties and slope position in a lowland rain forest of southern Taiwan. *Geoderma*, 123, 131–142. <https://doi.org/10.1016/j.geoderma.2004.01.031>



Urban, O., Janouš, D., Acosta, M. and Marek, M.E. (2007) Ecophysiological controls over the net ecosystem exchange of mountain spruce stand. Comparison of the response in direct vs. diffuse solar radiation. *Global Change Biology*, 13, 157–168. <https://doi.org/10.1111/j.1365-2486.2006.01265.x>

von Uexküll, H.R. and Mutert, E. (1995) Global extent, development and economic impact of acid soils. *Plant and Soil*, 171, 1–15. <https://doi.org/10.1007/BF00009558>

Zelený, D. (2021) *twinspanR: TTwo-way INdicator SPecies ANalysis (and its modified version) in R. Version 0.22. Available at <https://github.com/zdealveindy/twinspanR> [Accessed 3 October 2021]*

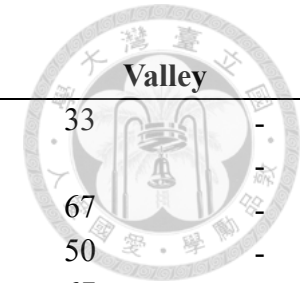


Appendices

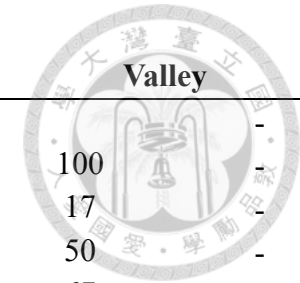
Appendix 1: Synoptic table

Table S1. Diagnostic species of the three vegetation types. Values are the relative percentage frequency and species are sorted by decreasing fidelity (Φ). The green color indicates diagnostic species with the fidelity $\geq 35\%$.

Vegetation type No. of plots Species	Ridge 74		East-facing slope 20		Valley 6	
	Frequency	Fidelity	Frequency	Fidelity	Frequency	Fidelity
<i>Daphniphyllum himalayense</i> subsp. <i>macropodum</i>	62	38.1	30	33	17	-
<i>Rhododendron formosanum</i>	93	37.9	95	-	17	-
<i>Pourthiaea villosa</i> var. <i>parvifolia</i>	7	-	75	75.8	-	-
<i>Eurya glaberrima</i>	61	-	95	60.9	-	-
<i>Viburnum luzonicum</i>	11	-	50	52.3	-	-
<i>Quercus stenophylloides</i>	-	-	35	51.4	-	-
<i>Microtropis fokienensis</i>	12	-	50	51.1	-	-
<i>Osmanthus heterophyllus</i>	32	-	70	43.8	17	-
<i>Tetradium ruticarpum</i>	-	-	25	42.6	-	-
<i>Ilex sugerokii</i> var. <i>brevipedunculata</i>	4	-	30	41.6	-	-
<i>Itea parviflora</i>	3	-	25	38.5	-	-
<i>Litsea elongata</i> var. <i>mushaensis</i>	38	-	90	37.3	67	-
<i>Skimmia japonica</i> subsp. <i>distincte-venulosa</i>	4	-	25	36.6	-	-
<i>Hydrangea angustipetala</i>	3	-	-	-	33	46.4
<i>Eurya loquaiana</i>	7	-	10	-	-	-



Vegetation type	Ridge		East-facing slope		Valley	
<i>Chamaecyparis obtusa</i> var. <i>formosana</i>	85	-	90	-	33	-
<i>Tsuga chinensis</i> var. <i>formosana</i>	3	-	-	-	-	-
<i>Neolitsea acuminatissima</i>	88	-	95	-	67	-
<i>Trochodendron aralioides</i>	95	34.2	75	-	50	-
<i>Cleyera japonica</i>	81	-	75	-	67	-
<i>Ilex lonicerifolia</i>	12	-	30	20.5	17	-
<i>Pourthiaea beauverdiana</i> var. <i>notabilis</i>	-	-	5	-	-	-
<i>Euonymus spraguei</i>	-	-	5	-	-	-
<i>Dendropanax dentiger</i>	62	-	70	-	50	-
<i>Prunus transarisanensis</i>	38	-	55	-	-	-
<i>Schima superba</i>	1	-	-	-	-	-
<i>Acer morrisonense</i>	1	-	-	-	-	-
<i>Michelia compressa</i>	3	-	5	-	-	-
<i>Litsea acuminata</i>	8	-	5	-	17	-
<i>Lindera erythrocarpa</i>	11	-	10	-	-	-
<i>Photinia nitakayamensis</i>	8	-	-	-	-	-
<i>Acer kawakamii</i>	8	-	10	-	-	-
<i>Quercus sessilifolia</i>	72	-	90	-	83	-
<i>Sycopsis sinensis</i>	5	-	5	-	17	-
<i>Rhamnus crenata</i>	8	-	5	-	-	-
<i>Neolitsea aciculata</i>	9	-	5	-	-	-
<i>Styrax formosanus</i>	14	-	10	-	-	-
<i>Machilus thunbergii</i>	3	-	-	-	-	-
<i>Acer palmatum</i> var. <i>pubescens</i>	35	-	50	-	33	-



Vegetation type	Ridge		East-facing slope		Valley	
<i>Ilex tugitakayamensis</i>	30	-	35	-	-	-
<i>Symplocos macrostroma</i>	72	-	100	22.9	100	-
<i>Carpinus rankanensis</i>	4	-	30	24.7	17	-
<i>Symplocos formosana</i>	16	-	60	25.7	50	-
<i>Ligustrum liukiense</i>	53	-	80	20.3	67	-
<i>Eurya crenatifolia</i>	73	-	100	22.2	100	-
<i>Ilex suzukii</i>		-	10	26.3		-
<i>Viburnum foetidum</i> var. <i>rectangulatum</i>		-	15	32.4		-
<i>Sorbus randaiensis</i>	3	-	20	33.2		-
<i>Barthea barthei</i>	3	-	20	33.2		-
<i>Viburnum urceolatum</i>		-	10	26.3		-
<i>Ilex hayatana</i>	31	-	55	30.9	17	-
<i>Camellia brevistyla</i>	39	-	85	31.4	67	-
<i>Rhododendron leptosanthurum</i>	1	-		-		-
<i>Tetradium glabrifolium</i>	1	-		-		-
<i>Viburnum sympodiale</i>	27	-	40	-	17	-
<i>Quercus longinux</i>	26	-	45	-		-
<i>Vaccinium bracteatum</i>	1	-		-		-
<i>Rhododendron pseudochrysanthurum</i>	1	-		-		-
<i>Prunus phaeosticta</i>	23	-	35	-	67	-
<i>Berberis hayatana</i>		-	5	-		-
<i>Symplocos migoii</i>		-		-	17	-
<i>Callicarpa randaiensis</i>	5	-	30	11.9	33	-
<i>Pieris taiwanensis</i>	1	-		-		-

Vegetation type	Ridge	East-facing slope	Valley
<i>Benthamidia japonica</i> var. <i>chinensis</i>	1	-	-
<i>Chamaecyparis formosensis</i>	1	10	-



Appendix 2: The differences between the selected soil chemical properties in DCA

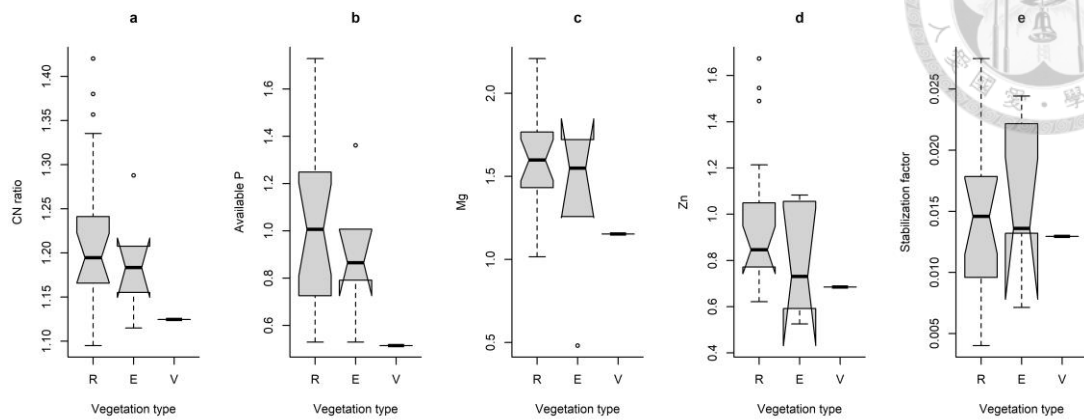


Figure S1. Boxplots showing the differences of the soil chemical properties selected in the DCA ordination diagram (only containing data from the 25 selected subplots, where 18 subplots belong to ridge type, 6 subplots belong to east-facing slope type, and 1 subplot belongs to valley type) between the three vegetation types. None of the boxplots were tested significant between different vegetation types (a. C/N ratio, b. available P, c. Mg, d. Zn, e. stabilization factor); R: ridge type, E: east-facing slope type, V: valley type.

Appendix 3: Correlations between environmental variables

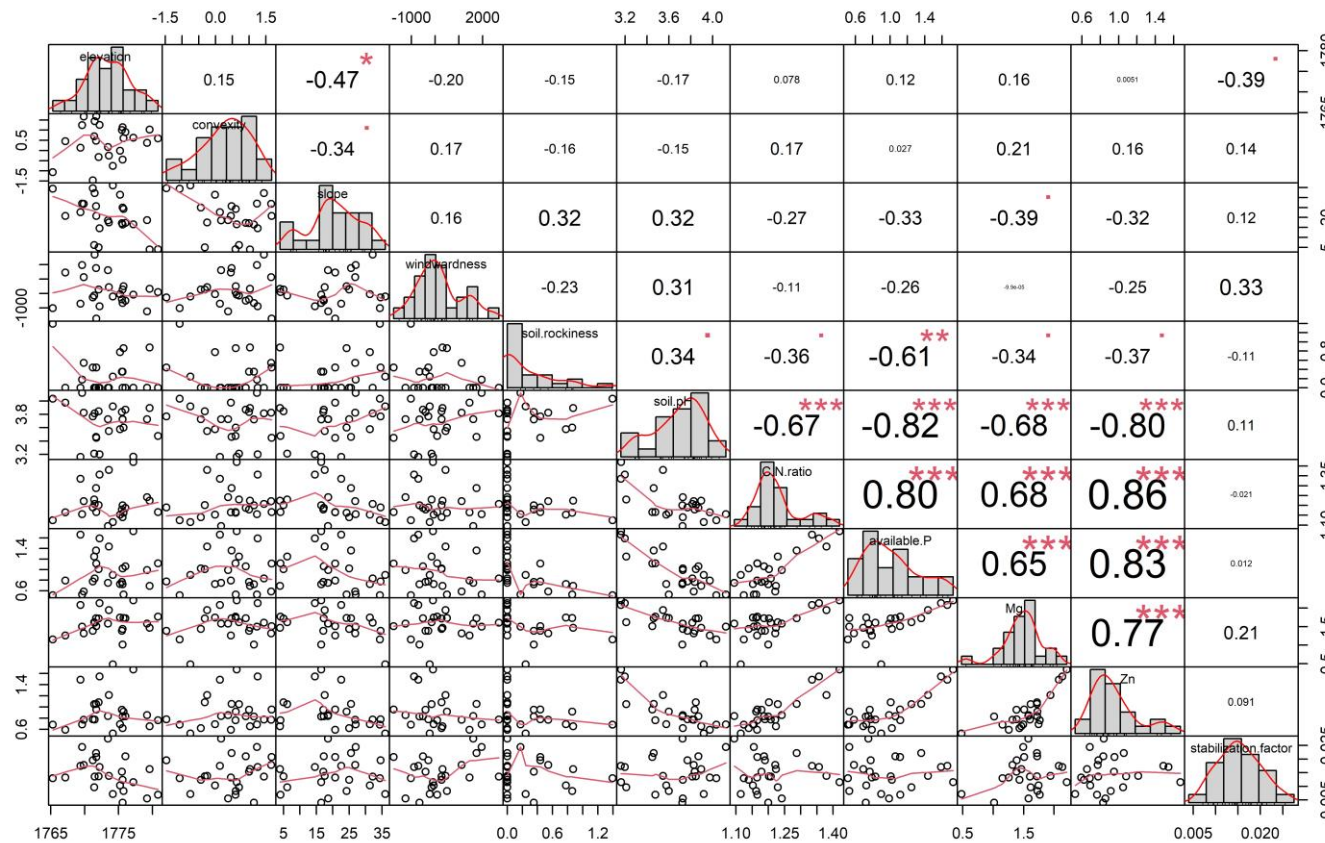
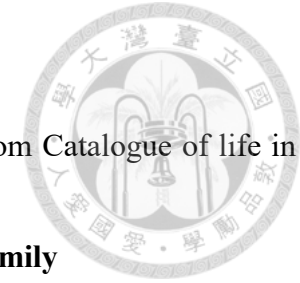


Figure S2. Correlation of significant topographical and soil properties variables. Panels in the upper triangle show correlation coefficients with results of significance testing (‘***’: $P < 0.001$, ‘**’: $P < 0.01$, ‘*’: $P < 0.05$, ‘.’ $P < 0.1$, i.e. marginally significant). Panels on diagonal show histograms of distribution. Panels on lower triangle show scatterplot with loess smoother curve.



Appendix 4: Species checklist

Table S2. Checklist for all woody species (excluding lianas) in LFDP. Arranged by alphabetic order of species name from Catalogue of life in Taiwan (TaiCoL, <https://taibnet.sinica.edu.tw/>).

Latin name	Chinese name	Family
<i>Acer kawakamii</i>	尖葉槭	Aceraceae
<i>Acer morrisonense</i>	臺灣紅榨槭	Aceraceae
<i>Acer palmatum</i> var. <i>pubescens</i>	臺灣掌葉槭	Aceraceae
<i>Barthea barthei</i>	深山野牡丹	Melastomataceae
<i>Benthamidia japonica</i> var. <i>chinensis</i>	四照花	Cornaceae
<i>Berberis hayatana</i>	早田氏小檗	Berberidaceae
<i>Callicarpa randaiensis</i>	巒大紫珠	Verbenaceae
<i>Camellia brevistyla</i>	短柱山茶	Theaceae
<i>Carpinus rankanensis</i>	蘭邯千金榆	Betulaceae
<i>Chamaecyparis formosensis</i>	紅檜	Cupressaceae
<i>Chamaecyparis obtusa</i> var. <i>formosana</i>	臺灣扁柏	Cupressaceae
<i>Cleyera japonica</i>	紅淡比	Theaceae
<i>Daphniphyllum himalayense</i> subsp. <i>macropodium</i>	薄葉虎皮楠	Daphniphyllaceae

Latin name	Chinese name	Family
<i>Dendropanax dentiger</i>	臺灣樹參	Araliaceae
<i>Euonymus spraguei</i>	刺果衛矛	Celastraceae
<i>Eurya crenatifolia</i>	假柃木	Theaceae
<i>Eurya glaberrima</i>	厚葉柃木	Theaceae
<i>Eurya loquaiana</i>	細枝柃木	Theaceae
<i>Hydrangea angustipetala</i>	狹瓣八仙花	Saxifragaceae
<i>Ilex hayatana</i>	早田氏冬青	Aquifoliaceae
<i>Ilex lonicerifolia</i>	忍冬葉冬青	Aquifoliaceae
<i>Ilex sugerokii</i> var. <i>brevipedunculata</i>	太平山冬青	Aquifoliaceae
<i>Ilex suzukii</i>	鈴木冬青	Aquifoliaceae
<i>Ilex tugitakayamensis</i>	雪山冬青	Aquifoliaceae
<i>Itea parviflora</i>	小花鼠刺	Saxifragaceae
<i>Ligustrum liukiense</i>	日本女貞	Oleaceae
<i>Lindera erythrocarpa</i>	鐵釘樹	Lauraceae
<i>Litsea acuminata</i>	長葉木薑子	Lauraceae
<i>Litsea elongata</i> var. <i>mushaensis</i>	霧社木薑子	Lauraceae



Latin name	Chinese name	Family
<i>Machilus thunbergii</i>	紅楠	Lauraceae
<i>Michelia compressa</i>	烏心石	Magnoliaceae
<i>Microtropis fokienensis</i>	福建賽衛矛	Celastraceae
<i>Neolitsea aciculata</i>	銳葉新木薑子	Lauraceae
<i>Neolitsea acuminatissima</i>	高山新木薑子	Lauraceae
<i>Osmanthus heterophyllus</i>	異葉木犀	Oleaceae
<i>Photinia nitakayamensis</i>	玉山假沙梨	Rosaceae
<i>Pieris taiwanensis</i>	臺灣馬醉木	Ericaceae
<i>Pourthiaea beauverdiana</i> var. <i>notabilis</i>	臺灣老葉兒樹	Rosaceae
<i>Pourthiaea villosa</i> var. <i>parvifolia</i>	小葉石楠	Rosaceae
<i>Prunus phaeosticta</i>	墨點櫻桃	Rosaceae
<i>Prunus transarisanensis</i>	阿里山櫻花	Rosaceae
<i>Quercus longinux</i>	錐果櫟	Fagaceae
<i>Quercus sessilifolia</i>	毬子櫟	Fagaceae
<i>Quercus stenophylloides</i>	狹葉櫟	Fagaceae
<i>Rhamnus crenata</i>	鈍齒鼠李	Rhamnaceae



Latin name	Chinese name	Family
<i>Rhododendron formosanum</i>	臺灣杜鵑	Ericaceae
<i>Rhododendron leptosanthurum</i>	西施花	Ericaceae
<i>Rhododendron pseudochrysanthum</i>	玉山杜鵑	Ericaceae
<i>Schima superba</i>	木荷	Theaceae
<i>Skimmia japonica</i> subsp. <i>distincte-venulosa</i>	臺灣茵芋	Rutaceae
<i>Sorbus randaiensis</i>	巒大花楸	Rosaceae
<i>Styrax formosanus</i>	烏皮九芎	Styracaceae
<i>Sycopsis sinensis</i>	水絲梨	Hamamelidaceae
<i>Symplocos formosana</i>	臺灣灰木	Symplocaceae
<i>Symplocos macrostroma</i>	大花灰木	Symplocaceae
<i>Symplocos migoi</i>	擬日本灰木	Symplocaceae
<i>Tetradium glabrifolium</i>	賊仔樹	Rutaceae
<i>Tetradium ruticarpum</i>	吳茱萸	Rutaceae
<i>Trochodendron aralioides</i>	昆欄樹	Trochodendraceae
<i>Tsuga chinensis</i> var. <i>formosana</i>	臺灣鐵杉	Pinaceae
<i>Vaccinium bracteatum</i>	米飯花	Ericaceae



Latin name**Chinese name****Family***Viburnum foetidum* var. *rectangulatum*

狹葉莢蒾

Caprifoliaceae

Viburnum luzonicum

呂宋莢蒾

Caprifoliaceae

Viburnum sympodiale

假繡球

Caprifoliaceae

Viburnum urceolatum

壺花莢蒾

Caprifoliaceae



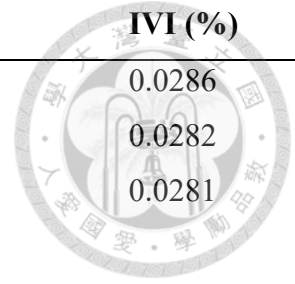
Appendix 5: Species IVI in LFDP

Table S3. List of species IVI in whole plot level. Arranged by decreasing IVI (%).

No.	Species	IVI (%)
1.	<i>Rhododendron formosanum</i>	14.4857
2.	<i>Chamaecyparis obtusa</i> var. <i>formosana</i>	13.9097
3.	<i>Quercus sessilifolia</i>	8.6768
4.	<i>Trochodendron aralioides</i>	6.5851
5.	<i>Eurya crenatifolia</i>	5.2935
6.	<i>Symplocos macrostroma</i>	4.9422
7.	<i>Cleyera japonica</i>	4.5571
8.	<i>Neolitsea acuminatissima</i>	4.3556
9.	<i>Eurya glaberrima</i>	3.6245
10.	<i>Daphniphyllum himalayense</i> subsp. <i>macropodum</i>	2.5123
11.	<i>Prunus transarisanensis</i>	2.4737
12.	<i>Ligustrum liukuense</i>	2.4142
13.	<i>Camellia brevistyla</i>	2.3052
14.	<i>Dendropanax dentiger</i>	2.2660
15.	<i>Quercus longinux</i>	2.1917
16.	<i>Osmanthus heterophyllus</i>	1.8956
17.	<i>Litsea elongata</i> var. <i>mushaensis</i>	1.8529
18.	<i>Acer palmatum</i> var. <i>pubescens</i>	1.4763
19.	<i>Pourthiaea villosa</i> var. <i>parvifolia</i>	1.2593
20.	<i>Ilex hayatana</i>	1.1787
21.	<i>Ilex tugitakayamensis</i>	1.0832
22.	<i>Viburnum sympodiale</i>	1.0128
23.	<i>Prunus phaeosticta</i>	1.0045
24.	<i>Symplocos formosana</i>	0.9114
25.	<i>Microtropis fokienensis</i>	0.6137
26.	<i>Viburnum luzonicum</i>	0.6028
27.	<i>Ilex lonicerifolia</i>	0.4972
28.	<i>Styrax formosanus</i>	0.4921
29.	<i>Callicarpa randaiensis</i>	0.3571
30.	<i>Quercus stenophylloides</i>	0.3545

No.	Species	IVI (%)
31.	<i>Carpinus rankanensis</i>	0.3370
32.	<i>Lindera erythrocarpa</i>	0.3330
33.	<i>Ilex sugerokii</i> var. <i>brevipedunculata</i>	0.2890
34.	<i>Acer kawakamii</i>	0.2805
35.	<i>Skimmia japonica</i> subsp. <i>distincte-venulosa</i>	0.2457
36.	<i>Sycopsis sinensis</i>	0.2420
37.	<i>Rhamnus crenata</i>	0.2374
38.	<i>Litsea acuminata</i>	0.2356
39.	<i>Neolitsea aciculata</i>	0.2325
40.	<i>Itea parviflora</i>	0.2182
41.	<i>Eurya loquaiana</i>	0.2129
42.	<i>Sorbus randaiensis</i>	0.1955
43.	<i>Photinia niitakayamensis</i>	0.1825
44.	<i>Barthea barthei</i>	0.1764
45.	<i>Tsuga chinensis</i> var. <i>formosana</i>	0.1638
46.	<i>Hydrangea angustipetala</i>	0.1635
47.	<i>Tetradium ruticarpum</i>	0.1144
48.	<i>Michelia compressa</i>	0.1053
49.	<i>Viburnum foetidum</i> var. <i>rectangulatum</i>	0.0978
50.	<i>Chamaecyparis formosensis</i>	0.0977
51.	<i>Machilus thunbergii</i>	0.0707
52.	<i>Viburnum urceolatum</i>	0.0626
53.	<i>Ilex suzukii</i>	0.0600
54.	<i>Tetradium glabrifolium</i>	0.0585
55.	<i>Vaccinium bracteatum</i>	0.0581
56.	<i>Rhododendron leptosanctum</i>	0.0474
57.	<i>Schima superba</i>	0.0452
58.	<i>Pieris taiwanensis</i>	0.0347
59.	<i>Rhododendron pseudochrysanctum</i>	0.0346
60.	<i>Pourthiaea beauverdiana</i> var. <i>notabilis</i>	0.0346
61.	<i>Euonymus spraguei</i>	0.0330
62.	<i>Benthamidia japonica</i> var. <i>chinensis</i>	0.0299

No.	Species	IVI (%)
63.	<i>Symplocos migoii</i>	0.0286
64.	<i>Acer morrisonense</i>	0.0282
65.	<i>Berberis hayatana</i>	0.0281



Appendix 6: R code



```
library(adespatial)
library(agricolae)
library(RColorBrewer)
library(fgeo)
library(multcomp)
library(twinspanR)
library(vegan)
library(Hmisc)
library(PerformanceAnalytics)
library(tidyverse)
library(dplyr)

setwd ('P:/Personal/Chen Ting/Master thesis/Data')

#species composition data----
spe_raw <- read.csv('species_composition_20210804.csv')
spe <- spe_raw %>%
  mutate (ba = (dbh / 2)^2 * pi) %>%
  group_by (individual) %>%
  summarise (quadrat = unique (quadrat),
            species_latin = unique (species_latin),
            ba = sum (ba)) %>%
  group_by (quadrat, species_latin) %>%
  summarise (ba = sum (ba),
            density = n()) %>%
  group_by (quadrat) %>%
  mutate (rel.ba = ba / sum (ba),
          rel.density = density / sum (density),
          IVI = (rel.ba + rel.density) / 2) %>%
  dplyr::select (quadrat, species_latin, IVI) %>%
  spread (key = species_latin, value = IVI, fill = 0) %>%
  column_to_rownames ('quadrat')
spe <- spe*100

#cluster analysis----
twinspan <- twinspan(spe, modif = T, clusters = 3)
cluster <- cut(twinspan)

#environmental factors----
pile <- read.csv ('LPP.pile.elevation.csv', stringsAsFactors =
F)
pile <- pile %>%
  mutate (x = x * 10,
          y = y * 10)
topo <- fgeo_topography (pile, gridsize = 10, xdim = 100, ydim
= 100, edgecorrect = T)
fx <- vector (mode = 'numeric')
fy <- vector (mode = 'numeric')
for (i in 0:109) {
  if (i %% 11 == 0) next
  fx [i] <- mean (pile$elevation [c(i + 11, i + 12)]) - mean
(pile$elevation [c(i, i + 1)])
}
```

```

fx <- fx [!is.na (fx)]
for (j in 0:109) {
  if (j %% 11 == 0) next
  fy [j] <- mean (pile$elevation [c(j + 1, j + 12)]) - mean
(pile$elevation [c(j, j + 11)])
}
fy <- fy [!is.na (fy)]
# fx [62] == 0, set a small number for it.
fx [62] <- 0.0001
aspect <- 180 - (atan (fy / fx)*(180 / pi)) + 90*(fx / abs (fx))
topo <- topo %>%
  mutate (aspect = aspect,
          subplot = paste0 ('(', gx / 10, ',', gy / 10, ')')) %>%
  transmute (subplot = subplot,
            elevation = meanelev,
            convexity = convex,
            slope = slope,
            aspect = aspect)
#write.csv (topo, 'topo.csv', row.names = F)
#merged cluster analysis result and soil properties data with
topographical variables, and save into new file
'environmental_factors_20221214.csv'.
env <- read.csv(file = 'environmental_factors_20230215.csv',
row.names = 1)
env$C <- log10(env$C)
env$tN <- log10(env$tN)
env$C.N.ratio <- log10(env$C.N.ratio)
env$eN <- log10(env$eN)
env$available.P <- log10(env$available.P)
env$K <- log10(env$K)
env$Ca <- log10(env$Ca)
env$Mg <- log10(env$Mg)
env$Cu <- log10(env$Cu*100)
env$Zn <- log10(env$Zn)
env$stabilization.factor <- (env$stabilization.factor)^2
env$decomposition.rate <- log10(env$decomposition.rate*1000)

#physiognomical variables----
spe_raw$ba <- ((spe_raw$dbh/2)^2)*pi
ivi_total_ba <- spe_raw %>% group_by (quadrat) %>% summarise(BA
= sum(ba) / 100)
individual <- read.csv('individual_data_20230103.csv')
individual$number <- 1
quadrat_individual <- individual %>% group_by(quadrat) %>%
summarise(individual = sum(number))
quadrat_individual <- cbind(quadrat_individual, cluster)
mean_BA <- (ivi_total_ba$BA*100) /
quadrat_individual$individual
mean_DBH <- sqrt(mean_BA / pi)*2
quadrat_ba <- cbind(ivi_total_ba, mean_DBH, cluster)
quadrat_species <- individual %>% group_by(quadrat,
species_latin) %>% summarise(total = sum(number))
quadrat_species$number <- 1
quadrat_richness <- quadrat_species %>% group_by(quadrat) %>%
summarise(richness = sum(number))
quadrat_richness <- cbind(quadrat_richness, cluster)

```



```

leaf_type_ba <- read.csv('leaf_type_ba_20221205.csv')
ltba <- leaf_type_ba %>%
  mutate (ba = (DBH / 2)^2 * pi) %>%
  group_by (individual) %>%
  summarise (subplot = unique (subplot),
            leaf.style = unique (leaf.style),
            ba = sum (ba)) %>%
  group_by (subplot, leaf.style) %>%
  summarise (ba = sum (ba)/100) %>%
  dplyr::select (subplot, leaf.style, ba) %>%
  spread (key = leaf.style, value = ba, fill = 0) %>%
  column_to_rownames ('subplot')
ltba <- cbind(ltba, cluster)
quadrat_ba$cluster <- as.factor(quadrat_ba$cluster)
quadrat_individual$cluster <- as.factor(quadrat_individual$cluster)
quadrat_richness$cluster <- as.factor(quadrat_richness$cluster)
ltba$cluster <- as.factor(ltba$cluster)

anova_test <- aov(BA ~ cluster, data = quadrat_ba)
summary(anova_test)
phy_grp <- HSD.test(anova_test, "cluster", group = T)
phy_grp
anova_test <- aov(mean_DBH ~ cluster, data = quadrat_ba)
summary(anova_test)
phy_grp <- HSD.test(anova_test, "cluster", group = T)
phy_grp
anova_test <- aov(individual ~ cluster, data = quadrat_individual)
summary(anova_test)
phy_grp <- HSD.test(anova_test, "cluster", group = T)
phy_grp
anova_test <- aov(richness ~ cluster, data = quadrat_richness)
summary(anova_test)
phy_grp <- HSD.test(anova_test, "cluster", group = T)
phy_grp
anova_test <- aov(Conifer ~ cluster, data = ltba)
summary(anova_test)
phy_grp <- HSD.test(anova_test, "cluster", group = T)
phy_grp
anova_test <- aov(Evergreen ~ cluster, data = ltba)
summary(anova_test)
phy_grp <- HSD.test(anova_test, "cluster", group = T)
phy_grp
anova_test <- aov(Deciduous ~ cluster, data = ltba)
summary(anova_test)

#physiognomy boxplot----
quadrat_ba$veg.type <- cluster
quadrat_ba[quadrat_ba$veg.type == 1, 5] <- 'R'
quadrat_ba[quadrat_ba$veg.type == 2, 5] <- 'E'
quadrat_ba[quadrat_ba$veg.type == 3, 5] <- 'V'
quadrat_individual$veg.type <- cluster
quadrat_individual[quadrat_individual$veg.type == 1, 4] <- 'R'
quadrat_individual[quadrat_individual$veg.type == 2, 4] <- 'E'
quadrat_individual[quadrat_individual$veg.type == 3, 4] <- 'V'

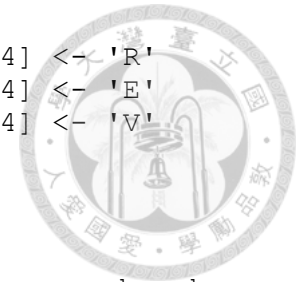
```



```

quadrat_richness$veg.type <- cluster
quadrat_richness[quadrat_richness$veg.type == 1, 4] <- 'R'
quadrat_richness[quadrat_richness$veg.type == 2, 4] <- 'E'
quadrat_richness[quadrat_richness$veg.type == 3, 4] <- 'V'
ltba$veg.type <- cluster
ltba[ltba$veg.type == 1, 5] <- 'R'
ltba[ltba$veg.type == 2, 5] <- 'E'
ltba[ltba$veg.type == 3, 5] <- 'V'
quadrat_ba$veg.type <- factor(quadrat_ba$veg.type, ordered =
TRUE, levels = c('R', 'E', 'V'))
quadrat_individual$veg.type <-
factor(quadrat_individual$veg.type, ordered = TRUE, levels =
c('R', 'E', 'V'))
quadrat_richness$veg.type <- factor(quadrat_richness$veg.type,
ordered = TRUE, levels = c('R', 'E', 'V'))
ltba$veg.type <- factor(ltba$veg.type, ordered = TRUE, levels =
c('R', 'E', 'V'))
jpeg (filename = 'physiognomical_boxplot.jpg', width = 10,
height = 6.5, units = "in", res = 600, quality = 100)
par(mfrow=c(2,4))
boxplot(BA ~ veg.type, data = quadrat_ba, xlab = 'Vegetation
type', ylab = 'BA [m2 ha-1]', main = 'a', frame = F, notch =
TRUE, ylim = c(0, 240))
box(bty = 'l')
text(x = c(1, 2, 3), y = 230, labels = c('a', 'a', 'b'))
boxplot(mean_DBH ~ veg.type, data = quadrat_ba, xlab =
'Vegetation type', ylab = 'Mean DBH [cm]', main = 'b', frame =
F, notch = TRUE, ylim = c(0, 34))
box(bty = 'l')
text(x = c(1, 2, 3), y = 33, labels = c('a', 'b', 'ab'))
boxplot(individual ~ veg.type, data = quadrat_individual, xlab =
'Vegetation type', ylab = 'Density', main = 'c', frame = F,
notch = TRUE, ylim = c(0, 220))
box(bty = 'l')
text(x = c(1, 2, 3), y = 210, labels = c('b', 'a', 'b'))
boxplot(richness ~ veg.type, data = quadrat_richness, xlab =
'Vegetation type', ylab = 'Species richness', main = 'd', frame
= F, notch = TRUE, ylim = c(0, 37))
box(bty = 'l')
text(x = c(1, 2, 3), y = 35, labels = c('b', 'a', 'b'))
boxplot(Conifer ~ veg.type, data = ltba, xlab = 'Vegetation type',
ylab = 'BA of conifer species [m2 ha-1]', main = 'e', frame = F,
notch = TRUE, ylim = c(0, 190))
box(bty = 'l')
text(x = c(1, 2, 3), y = 170, labels = c('a', 'b', 'ab'))
boxplot(Evergreen ~ veg.type, data = ltba, xlab = 'Vegetation
type', ylab = 'BA of evergreen broadleaf species [m2 ha-1]',
main = 'f', frame = F, notch = TRUE, ylim = c(0, 135))
box(bty = 'l')
text(x = c(1, 2, 3), y = 130, labels = c('b', 'a', 'c'))
boxplot(Deciduous ~ veg.type, data = ltba, xlab = 'Vegetation
type', ylab = 'BA of deciduous broadleaf species [m2 ha-1]',
main = 'g', frame = F, notch = TRUE)
box(bty = 'l')
dev.off()

```




```

#env factors anova test----
env$cluster <- as.factor(env$cluster)
anova_test <- aov(elevation ~ cluster, data = env)
summary(anova_test)
phy_grp <- HSD.test(anova_test, "cluster", group = T)
phy_grp
anova_test <- aov(convexity ~ cluster, data = env)
summary(anova_test)
phy_grp <- HSD.test(anova_test, "cluster", group = T)
phy_grp
anova_test <- aov(slope ~ cluster, data = env)
summary(anova_test)
phy_grp <- HSD.test(anova_test, "cluster", group = T)
phy_grp
anova_test <- aov(windwardness ~ cluster, data = env)
summary(anova_test)
phy_grp <- HSD.test(anova_test, "cluster", group = T)
phy_grp
anova_test <- aov(soil.rockiness ~ cluster, data = env)
summary(anova_test)
phy_grp <- HSD.test(anova_test, "cluster", group = T)
phy_grp
anova_test <- aov(soil.pH ~ cluster, data = env)
summary(anova_test)
phy_grp <- HSD.test(anova_test, "cluster", group = T)
phy_grp
anova_test <- aov(soil.depth ~ cluster, data = env)
summary(anova_test)

#env factors boxplot----
env$veg.type <- factor(env$veg.type, ordered = TRUE, levels =
c('R', 'E', 'V'))
jpeg (filename = 'environmental_boxplot.jpg', width = 10, height
= 6.5, units = "in", res = 600, quality = 100)
par(mfrow=c(2,4))
boxplot(elevation ~ veg.type, data = env, xlab = 'Vegetation
type', ylab = 'Elevation [m a.s.l.]',main = 'a', frame = F, notch
= TRUE, ylim = c(1760, 1785))
box(bty = 'l')
text(x = c(1, 2, 3), y = 1782.5, labels = c('a', 'b', 'b'))
boxplot(convexity ~ veg.type, data = env, xlab = 'Vegetation
type', ylab = 'Convexity', main = 'b', frame = F, notch = TRUE,
ylim = c(-3, 3.5))
box(bty = 'l')
text(x = c(1, 2, 3), y = 3.1, labels = c('a', 'a', 'b'))
boxplot(slope ~ veg.type, data = env, xlab = 'Vegetation type',
ylab = 'Slope [°]', main = 'c', frame = F, notch = TRUE, ylim =
c(0, 50))
box(bty = 'l')
text(x = c(1, 2, 3), y = 48, labels = c('b', 'a', 'a'))
boxplot(windwardness ~ veg.type, data = env, xlab = 'Vegetation
type', ylab = 'Windwardness', main = 'd', frame = F, notch =
TRUE, ylim = c(-2000, 4000))
box(bty = 'l')
text(x = c(1, 2, 3), y = 3800, labels = c('b', 'a', 'b'))
boxplot(soil.rockiness ~ veg.type, data = env, xlab =

```



```

'Vegetation type', ylab = 'Soil rockiness [%]', main = 'e', frame
= F, notch = TRUE, ylim = c(-5, 30))
box(bty = 'l')
text(x = c(1, 2, 3), y = 28, labels = c('b', 'b', 'a'))
boxplot(soil.pH ~ veg.type, data = env, xlab = 'Vegetation type',
ylab = 'Soil pH', main = 'f', frame = F, notch = TRUE, ylim =
c(3.0, 4.5))
box(bty = 'l')
text(x = c(1, 2, 3), y = 4.4, labels = c('b', 'a', 'a'))
boxplot(soil.depth ~ veg.type, data = env, xlab = 'Vegetation
type', ylab = 'Soil depth', main = 'g', frame = F, notch = TRUE)
box(bty = 'l')
dev.off()
jpeg (filename = 'soil_chemical_boxplot.jpg', width = 10, height
= 4, units = "in", res = 600, quality = 100)
par(mfrow=c(1,5))
boxplot(C.N.ratio ~ veg.type, data = env, xlab = 'Vegetation
type', ylab = 'CN ratio',main = 'a', frame = F, notch = TRUE)
box(bty = 'l')
boxplot(available.P ~ veg.type, data = env, xlab = 'Vegetation
type', ylab = 'Available P', main = 'b', frame = F, notch = TRUE)
box(bty = 'l')
boxplot(Mg ~ veg.type, data = env, xlab = 'Vegetation type',
ylab = 'Mg', main = 'c', frame = F, notch = TRUE)
box(bty = 'l')
boxplot(Zn ~ veg.type, data = env, xlab = 'Vegetation type',
ylab = 'Zn', main = 'd', frame = F, notch = TRUE)
box(bty = 'l')
boxplot(stabilization.factor ~ veg.type, data = env, xlab =
'Vegetation type', ylab = 'Stabilization factor', main = 'e',
frame = F, notch = TRUE)
box(bty = 'l')
dev.off()

#DCA----
DCA <- decorana(spe)
colors <- c('#66c2a5', '#8da0cb', '#fc8d62')
colors <- colors[as.numeric(env$cluster)]
shapes <- c(15, 16, 17)
shapes <- shapes[as.numeric(env$cluster)]
jpeg (filename = 'DCA.jpg', width = 6.7, height = 6.7, units =
"in", res = 600, quality = 100)
ordiplot(DCA, display = 'si', type = 'n')
points(DCA, 'sites', col = colors, pch = shapes, cex = 1)
ef_topo <- envfit(DCA, env[,c(4:6,9:12)], permutations = how
(within = Within (type = 'grid', ncol = 10, nrow = 10, mirror =
TRUE), complete = TRUE))
ef_soil <- envfit(DCA, env[,c(13:29)], na.rm = T, permutations
= how (within = Within (type = 'grid', ncol = 5, nrow = 5, mirror
= TRUE), complete = TRUE))
plot(ef_topo, cex = 0.8, p.max = 0.05)
plot(ef_soil, cex = 0.8, col = 'red', p.max = 0.1)
legend("topright", legend = c('Ridge type', 'East-facing slope
type', 'Valley type'), col = c('#66c2a5', '#8da0cb', '#fc8d62'),
pch = c(15, 16, 17), cex = 1)
dev.off()

```

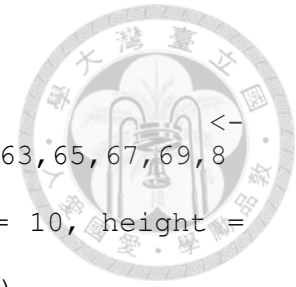
```

#correlation chart----
env$soil.rockiness <- log10(env$soil.rockiness+1)
env_cor <- c(1,3,5,7,9,21,23,25,27,29,41,43,45,47,49,61,63,65,67,69,81,83,85,87,89), c(4,5,6,9,11,12,18,20,23,27,28)]
jpeg (filename = 'correlation_chart.jpg', width = 10, height = 6.5, units = "in", res = 600, quality = 100)
chart.Correlation(env_cor, histogram=TRUE, pch=19)
dev.off()

#draw vegetation type map with elevation contour----
pile <- read.csv ('LPP.pile.elevation.csv', stringsAsFactors = F)
elevation.mat <- pile %>%
  mutate (x = x * 10,
           y = y * 10) %>%
  filter (x %in% seq (0, 100, 10)) %>%
  spread (key = x, value = elevation) %>%
  column_to_rownames (var = "y") %>%
  as.matrix () %>%
  t ()
colors <- c('#66c2a5', '#8da0cb', '#fc8d62', alpha = 0.7)
colors <- colors[as.numeric(env$cluster)]

jpeg (filename = 'vegetation_type_map.jpg', width = 6.7, height = 5.1, units = "in", res = 600, quality = 100)
layout (matrix (c(1, 2), ncol = 2), width = c(0.7, 0.3))
par (bg = 'white', fg = 'black',
      col.axis = 'black', col.lab = 'black', mar = c(3, 3, 1, 0),
      xpd = F)
contour (x = seq (0, 100, 10),
         y = seq (0, 100, 10),
         z = elevation.mat,
         xaxs = 'i', yaxs = 'i',
         xlab = 'Projected distance (m)',
         ylab = 'Projected distance (m)',
         lwd = 2, cex.axis = 0.8, tck = -0.015, mgp = c(2, 0.4, 0),
         add = FALSE)
points (x = sort (rep (seq (5, 95, 10), 10)),
        y = rep (seq (5, 95, 10), 10),
        pch = 22, cex = 8.6, col = 'grey', bg = colors)
contour (x = seq (0, 100, 10),
         y = seq (0, 100, 10),
         z = elevation.mat,
         xaxs = 'i', yaxs = 'i',
         xlab = 'Projected distance (m)',
         ylab = 'Projected distance (m)',
         lwd = 2, cex.axis = 0.8, tck = -0.015, mgp = c(2, 0.4, 0), col = 'grey10',
         add = TRUE)
par (xpd = T, mar = c(3, 0, 1, 0))
plot (x = 1, type = "n", axes = F, xlab = "", ylab = "")
legend ('bottomright', bty = 'n', inset = c(-0.04, 0), legend = c('Ridge type', 'East-facing slope type', 'Valley type'), pch =

```



```
15, pt.cex = 1.2, col = c('#66c2a5', '#8da0cb', '#fc8d62', alpha
= 0.7),
      y.intersp = 1.2)
dev.off()
```

